

# Origami Robots: Design, Actuation, and 3D Printing Methods

Wenbo Xue, Bingcong Jian,\* Liuchao Jin, Rong Wang, and Qi Ge\*

**Traditional robots, with their rigid structures and precise mechanical designs, have proven invaluable in industrial automation and structured environments but face challenges in dynamic and unstructured scenarios. Soft robots, composed of low-stiffness materials, offer adaptability and flexibility, making them ideal for applications like locomotion and minimally invasive surgery. However, their low load capacity and limited precision hinder their broader adoption.**

Origami robots emerge as a promising hybrid solution, combining the mechanical strength and precision of rigid robots with the adaptability and reconfigurability of soft robots. Leveraging the principles of origami, these robots employ rigid panels interconnected by flexible hinges, allowing for complex motions, structural transformations, and scalable designs while maintaining mechanical integrity. Traditional fabrication methods for origami robots, such as laser cutting and manual folding, limit their complexity and integration potential. However, advancements in 3D printing technologies, including Fused Deposition Modeling (FDM), Direct Ink Writing (DIW), Polyjet, and Two-Photon Polymerization (TPP), enable the creation of intricate geometries and multimaterial structures, significantly enhancing performance and broadening application domains. This review examines recent progress in origami robotic systems, focusing on their design, actuation mechanisms, fabrication techniques, and diverse applications, and concludes with future perspectives on leveraging advanced materials and manufacturing to drive innovation in the field.

## 1. Introduction

Traditional robots, characterized by rigid structures and precise mechanical designs, play a crucial role in industrial

automation, manufacturing, and structured environment operations.<sup>[1,2]</sup> These robots excel in tasks requiring high repeatability, accuracy, and strength, making them indispensable in assembly lines,<sup>[3]</sup> heavy-load operations,<sup>[4]</sup> and hazardous environments.<sup>[5]</sup> However, their rigidity limits adaptability and their design complexity hinders seamless integration into dynamic, unstructured environments, such as search-and-rescue missions or human-robot interaction scenarios. In contrast, soft robots, composed of low-stiffness materials, exhibit exceptional flexibility, adaptability, and safety when interacting with humans and delicate objects.<sup>[6]</sup> Their deformability enables navigation in complex environments and execution of tasks that rigid robots find challenging, making them suitable for applications such as locomotion,<sup>[7]</sup> flexible grasping,<sup>[8]</sup> minimally invasive surgery,<sup>[9]</sup> deep-sea exploration,<sup>[10]</sup> and biomedical devices.<sup>[11–15]</sup> However, the inherent low stiffness and nonlinear characteristics of soft materials impose

significant limitations on their functional capabilities. First, due to their inherently compliant nature, soft robots often exhibit low load-bearing capacity, which significantly restricts their ability to perform tasks involving lifting, pushing, or supporting external loads.<sup>[16]</sup> This structural softness, while beneficial for safe interaction, renders them unsuitable for applications that require mechanical strength and robustness. Second, the high degrees of freedom introduced by continuous deformation, combined with the nonlinear behavior of soft materials under actuation or external forces, pose substantial challenges for accurate modeling and control. Unlike rigid-body systems that follow well-established kinematic and dynamic models, soft robots often lack predictable behavior, making it difficult to design control algorithms for precise positioning or trajectory tracking.<sup>[17,18]</sup> These challenges restrict their use in scenarios requiring high precision, robustness, or complex dynamics. As a result, exploring a new type of robot that combines the advantages of rigid and flexible robots has become a significant research focus.

To overcome the limitations of soft robots—namely, low load-bearing capacity and difficulty in precise control due to nonlinear deformation—origami robots offer an effective hybrid solution that integrates rigid and flexible components. Origami robots

---

W. Xue, R. Wang, Q. Ge  
Shenzhen Key Laboratory for Additive Manufacturing of  
High-Performance Materials  
Department of Mechanical and Energy Engineering  
Southern University of Science and Technology  
Shenzhen 518055, China  
E-mail: [geq@sustech.edu.cn](mailto:geq@sustech.edu.cn)

B. Jian  
School of Mechanical Engineering  
Tongji University  
Shanghai 200092, China  
E-mail: [bingcongjian@tongji.edu.cn](mailto:bingcongjian@tongji.edu.cn)

L. Jin  
Department of Mechanical and Automation Engineering  
The Chinese University of Hong Kong  
Hong Kong, China

 The ORCID identification number(s) for the author(s) of this article can be found under <https://doi.org/10.1002/admt.202500278>

DOI: [10.1002/admt.202500278](https://doi.org/10.1002/admt.202500278)

emerge as a novel robotic paradigm that bridges the gap between rigid and soft robotics, leveraging the principles of origami, an ancient art of folding flat sheets into 3D structures.<sup>[19–21]</sup> Unlike conventional soft robots composed entirely of deformable materials, origami robots feature a body constructed from rigid panels, which provide high structural stiffness and significantly enhance their load-bearing capacity. This rigid framework allows the robot to withstand greater mechanical loads without compromising shape stability or performance, directly addressing the limitations of low load capacity in soft robots. Lee et al. developed a membrane-based origami transformable wheel capable of bearing loads over 10 kN, demonstrating that properly designed thick-membrane origami structures can achieve both high load capacity and adaptability, suitable for practical vehicular applications.<sup>[22]</sup> Park et al. propose a modular soft origami robotic system capable of high stiffness variation and demonstrated that their soft origami rover, utilizing facet buckling and pressurization, could carry a load of up to 14 kg, showcasing the remarkable load-bearing capacity of origami-based structures despite their lightweight and compact form.<sup>[23]</sup> In addition, the rigid-panel structure introduces a lower and more discrete number of degrees of freedom compared to the continuously deformable-body of soft robots. This reduction in configurational complexity not only facilitates more accurate mechanical modeling but also enables precise control strategies to be developed and implemented. As a result, the robot achieves higher positional accuracy and more reliable trajectory tracking, effectively overcoming the difficulties associated with nonlinear behavior and high-dimensional control in soft systems.<sup>[24–28]</sup> Wu et al. design a modular Kresling origami soft robot composed of segmental units, each with two discrete degrees of freedom—axial contraction and bending—enabling precise modeling and programmable control of locomotion and steering.<sup>[29]</sup> Xue et al. develop and precisely model an origami-based robotic gripper fabricated via hard–soft coupled multimaterial 3D printing, leveraging the panel–hinge structure's lower and more discrete number of degrees of freedom to enable accurate control and predictable motion behavior.<sup>[30]</sup> At the same time, the use of flexible creases—or hinges—ensures that the origami robot is not overly rigid. These creases introduce a certain degree of flexibility into the structure, allowing the robot to bend, twist, or deform in response to external forces or environmental interactions. This flexibility enables the origami robot to integrate the advantages of soft robotics, such as being more adaptable to complex and unstructured environments, exhibiting compliant behavior when in contact with objects or humans, and achieving versatile movement patterns. Moreover, their reliance on planar designs folded into 3D configurations significantly reduces manufacturing costs and expands material selection, offering enhanced flexibility and scalability.<sup>[31]</sup> Therefore, compared to soft robots, origami robots demonstrate superior load-bearing capacity and precise motion control due to their structural rigidity and reduced modeling complexity, effectively addressing the limitations of low payload capacity and nonlinear design challenges in soft robots.<sup>[32,33]</sup> The combination of foldable structures with flexible hinges bridges the gap between rigid mechanical systems and soft-bodied robots, resulting in robots that are both structurally programmable and mechanically resilient. These advantages spur the development of various origami robotic systems, including walking robots,<sup>[34,35]</sup> variable-wheel robots,<sup>[22,36]</sup> robotic

arms,<sup>[37,38]</sup> and crawling robots,<sup>[39,40]</sup> which are employed in applications spanning aerospace, architecture, medical devices, and environmental exploration.

Despite their potential, the fabrication of origami robots has heavily relied on traditional methods such as laser cutting, manual folding, and the layer-by-layer assembly of polymer or paper sheets.<sup>[34,41,42]</sup> While these approaches are effective for simple designs, they are labor-intensive and limited in their ability to produce intricate geometries or integrate multiple materials into a single structure. Moreover, these conventional techniques often fall short of fully utilizing the dynamic reconfigurability and advanced material properties necessary for optimizing the performance of origami robots. In response to these challenges, 3D printing emerges as a transformative technology in the fabrication of origami robots.<sup>[43–45]</sup> This advanced manufacturing technique enables the creation of complex geometries, freeform shapes, and multimaterial structures with high precision, effectively overcoming the constraints of traditional methods.<sup>[46,47]</sup> By allowing for the simultaneous printing of intricate designs and customizable material properties in a single build, 3D printing unlocks new possibilities for developing origami robots with superior performance, enhanced adaptability, and expanded application potential.<sup>[48,49]</sup> It is obvious that 3D-printed origami robots have generated remarkable impacts on practical applications. However, a systematic review on this topic is rare.

This paper provides a comprehensive review on recent advancements in origami-inspired robots, focusing on their design, actuation, and 3D printing methods along with their applications (**Figure 1**). Section 2 introduces various crease patterns, such as Yoshimura, Kresling, Miura, Flasher, and Water Bomb patterns, for folding various origami structures. Section 3 highlights actuation methods utilized to drive origami robots, such as pneumatic, cable-driven, magnetic, and smart material-based methods. Section 4 discusses the 3D printing technologies used to directly fabricate origami robots. These methods include Fused Deposition Modeling (FDM), Direct Ink Writing (DIW), Polyjet, Digital Light Processing (DLP), and Two-Photon Polymerization (TPP). Section 4 also provides a detailed discussion of the applications of the origami robots manufactured through 3D printing. Finally, Section 5 concludes this article and discusses the challenges that limit the 3D-printed origami robots from broader adoption, including 3D printing limitations, complex design processes, and the need for breakthrough applications, which highlights opportunities for innovation in material development, AI-assisted design, and real-world applications.

## 2. Crease Patterns and 3D Origami Structures

Origami offers boundless possibilities for creating 3D structures by precisely folding 2D sheets into special intricate 3D shapes.<sup>[50]</sup> Geometrically, through precisely designing crease patterns, origami enables the transformation of flat surfaces into approximate polyhedral geometries or smoothly curved 3D surfaces of any desired shape, with constant or variable curvature.<sup>[51]</sup> This highly versatile process makes origami an attractive method for fabricating advanced materials and robotic structures. **Figure 2** showcases five representative origami structures that are extensively studied and widely applied in robotic structures. Figure 2a,d,g,j,m presents the corresponding crease

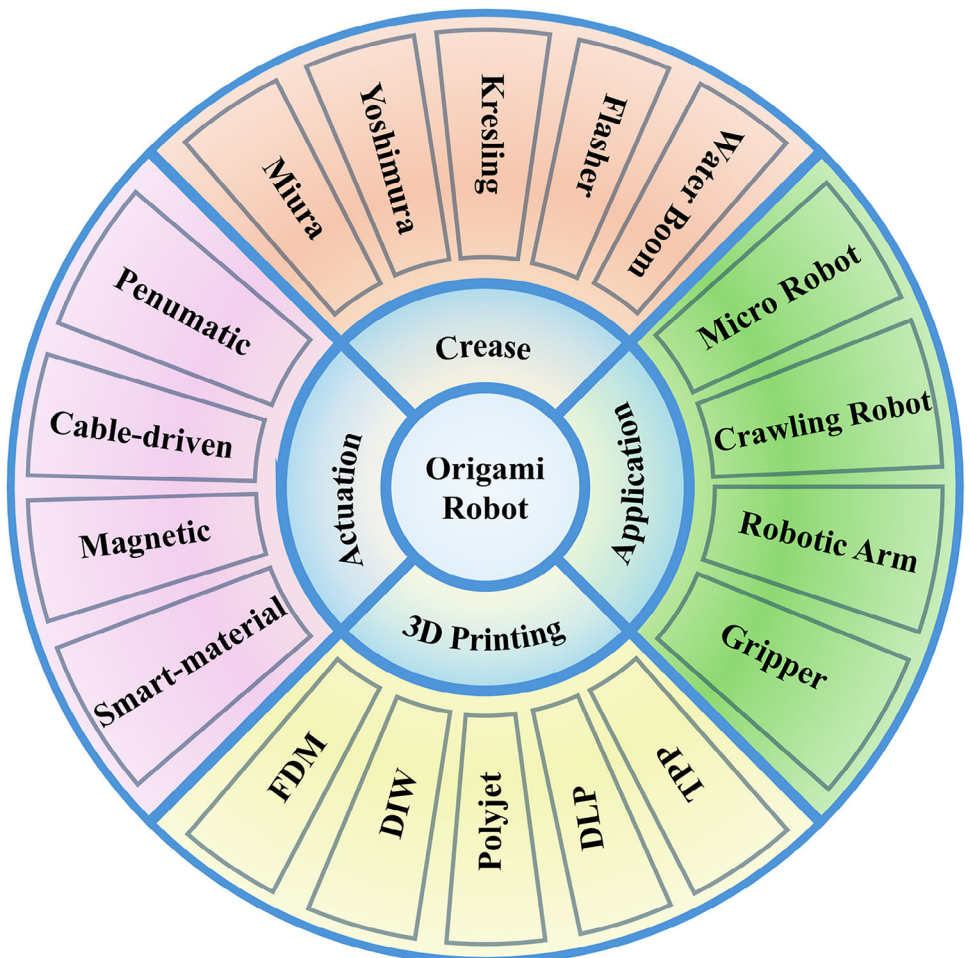


**Figure 1.** Overview on design, actuation, and 3D printing methods for origami robots.

pattern for folding these five origami structures, where the solid blue lines denote mountain folds (forming upward ridges) and dashed red lines denote valley folds (forming downward grooves).

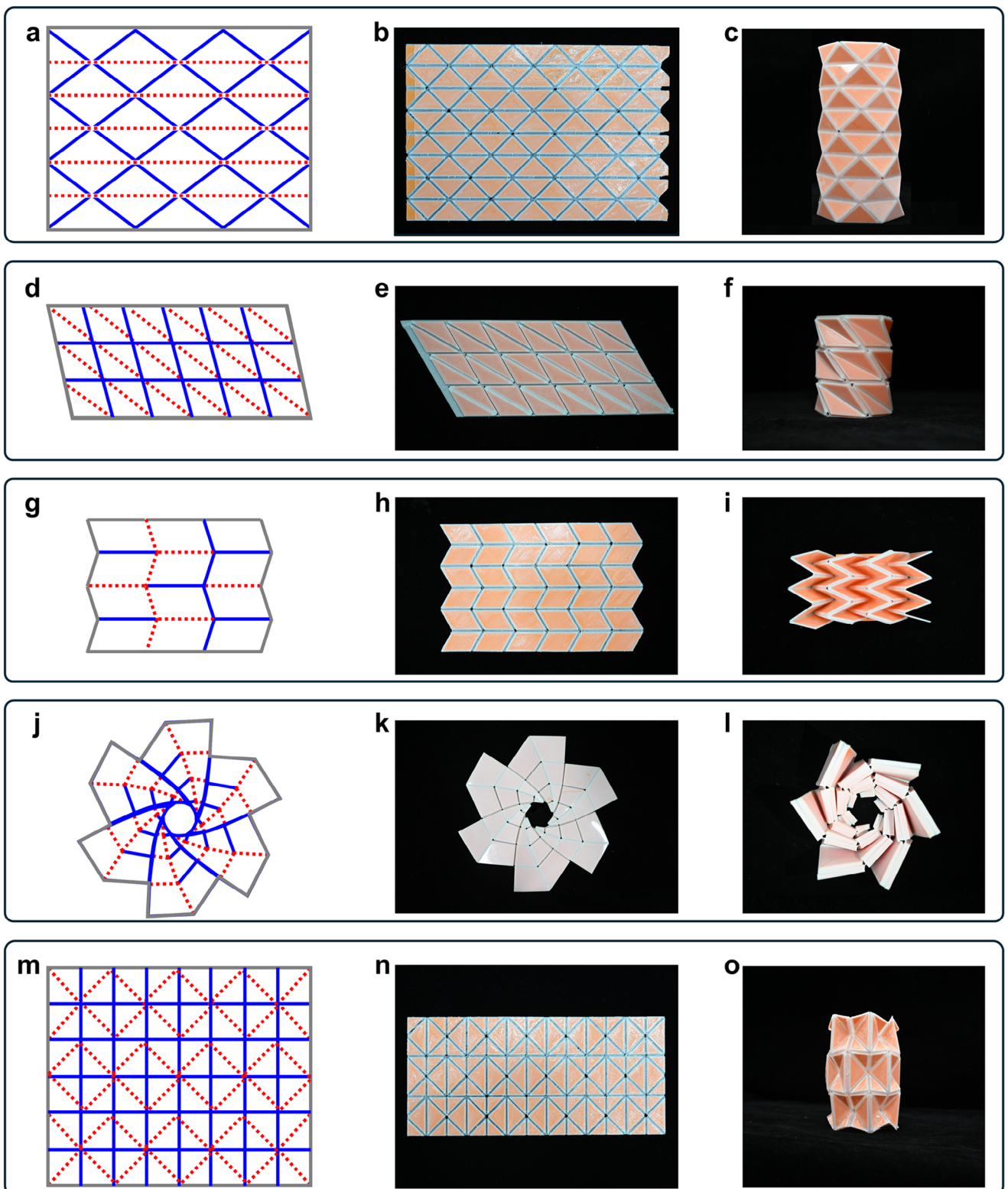
Detailed folding processes for each of these origami structures, including the Yoshimura, Kresling, Miura, six-sided Flasher, and Waterbomb patterns, can be found in the following references: Yoshimura folding process,<sup>[52]</sup> Kresling folding process,<sup>[53]</sup> Miura folding process,<sup>[54]</sup> six-sided Flasher folding process,<sup>[55]</sup> and Waterbomb folding process.<sup>[56]</sup>

Figure 2a presents the typical Yoshimura origami crease pattern, also referred to as the “diamond pattern.” This design features a diagonal folding pattern of rhombuses, where all diagonal creases are mountain folds. As shown in Figure 2b, a Yoshimura origami sheet fabricated using FDM multimaterial 3D printing technology can be folded to create a 3D cylindrical origami structure by folding the sheet and attaching the two side edges (Figure 2c). Due to high foldability under axial compression, cylindrical Yoshimura structures are employed in various applications such as robotic arms,<sup>[57,58]</sup> pipe robots,<sup>[33]</sup> and soft grippers.<sup>[58]</sup>

Figure 2d depicts the Kresling origami crease pattern, which consists of a matrix of parallelograms. In this pattern, the sides of each parallelogram serve as the mountain folds, while the longer

diagonal of each parallelogram represents the valley fold. Analogy to the Yoshimura pattern, the Kresling pattern can also be folded into a cylindrical structure by attaching the two side edges. A distinctive and unique feature of cylindrical Kresling structures is their ability to exhibit in-plane torsion under axial compression, making them particularly suited for applications requiring torsional stiffness, such as pump actuators<sup>[59]</sup> impact absorption tubes,<sup>[46]</sup> biomedical diagnoses and treatment robots.<sup>[60]</sup>

Figure 2g shows the Miura origami crease pattern, a classic rigid-foldable design extensively used in engineering for efficient folding. It consists of regular parallelogram units, each forming 4° vertices with alternating mountain and valley folds. The precise crease angles ensure synchronized movement during both folding and unfolding. The key feature of the Miura pattern lies in its periodic parallelogram arrangement, enabling smooth, unidirectional folding for efficient area transformation. This characteristic makes it particularly suitable for applications requiring high compression and rapid deployment, such as solar panels, compact maps, and packaging materials. Additionally, owing to its geometrically constrained design, the single-degree-of-freedom motion of Miura allows folding and unfolding with only one driving point, which is applied to develop locomotion robots<sup>[61]</sup> and robotic grippers.<sup>[62,63]</sup>



**Figure 2.** Crease patterns and 3D configurations of classical origami structures are designed and fabricated in this work. (a) Yoshimura origami crease pattern, (b) 3D-printed Yoshimura in planar form, (c) Assembled 3D Yoshimura structure; (d) Kresling origami crease pattern, (e) 3D-printed Kresling in planar form, (f) Assembled 3D Kresling structure; (g) Miura origami crease pattern, (h) 3D-printed Miura in planar form, (i) Assembled 3D Miura; (j) The six-sided Flasher origami crease pattern, (k) 3D-printed six-sided Flasher in planar form, (l) Assembled 3D six-sided Flasher structure; (m) Waterbomb origami crease pattern, (n) 3D-printed Waterbomb in planar form, (o) Assembled 3D Waterbomb structure.

As illustrated in Figure 2j, the six-sided Flasher demonstrates remarkable rotational symmetry and complex geometric characteristics. Each unit incorporates alternating mountain and valley folds, ensuring rigid foldability. The crease pattern radiates symmetrically from a central hexagon, with periodic and consistent folding arrangements in each sector. Specifically, in a six-sector ( $m = 6$ ) flasher, the central polygon is a regular hexagon, surrounded by radial crease distributions. Adding diagonal creases enhances the Flasher's rigid folding properties, enabling it to transition smoothly from a highly compact to a fully deployed configuration. Its high expansion-to-compression ratio makes it particularly suitable for deployable structures like space arrays, solar panels,<sup>[64]</sup> and deployable wheels,<sup>[65]</sup> where efficient storage and deployment are crucial.

As represented in Figure 2m, the Waterbomb pattern is a high-degree vertex design renowned for its ability to form robust 3D structures. The  $8^\circ$  vertices waterbomb configuration alternates between four mountain and four valley folds, while the  $6^\circ$  version implements four mountain folds integrated with two valley folds. When arranged with  $6^\circ$  vertices waterbomb units periodically, these units form the well-known "magic origami ball," showcasing exceptional versatility and rigidity. The Waterbomb pattern is particularly useful in deployable and adaptive applications requiring rapid expansion and compact folding, such as grippers,<sup>[62]</sup> deformable wheel robots,<sup>[22,66]</sup> and deployable stent grafts.<sup>[67]</sup>

Although the above crease patterns primarily reflect rigid-foldable origami principles, they often face limitations when integrated into soft-material-dominated or hybrid soft-rigid robotic systems. In such systems, achieving non-rigid or compliant foldability becomes crucial for preserving the flexibility and deformability of soft components. To address this challenge, recent studies have begun exploring crease patterns specifically tailored for soft-rigid integration. For example, variable stiffness crease networks and compliant mechanisms that incorporate elastomeric hinges or embedded soft joints are being developed to replace traditional sharp folds.<sup>[54]</sup> These emerging designs enable smooth curvature, tunable bending stiffness, and multi-mode deformations, thereby bridging the gap between structural compliance and geometric programmability. Such patterns have been applied to soft grippers, adaptive wearable devices, and morphing skins.<sup>[30]</sup> The development of hybrid crease designs marks an important advancement in expanding the applicability of origami robots to environments requiring both flexibility and robustness.

For scalability, the properties of crease patterns do not change significantly when scaled up or down, but the performance of origami robots may be affected by factors such as material selection, structural integrity, and the manufacturing process. For instance, while large-scale robots can take advantage of the same basic crease patterns, they may require more robust materials to maintain foldability and structural strength, whereas micro-scale robots may benefit from more precise fabrication techniques to achieve the required flexibility. The fabrication of both large and micro-scale origami robots presents unique challenges, with the latter requiring advanced micro-fabrication methods to achieve the small-scale precision necessary for complex fold geometries. Additionally, in large-scale applications, the limitations of current 3D printing technologies, such as resolution and material properties, will not affect the scalability of these systems.

### 3. Actuation Methods for Driving Origami Robots

Actuation is the key to converting static origami structures to origami robots. Figures 3–6 summarize the mainstream methods for actuating origami robots including pneumatic,<sup>[68–73]</sup> cable-driven,<sup>[74–76]</sup> magnetic,<sup>[77–79]</sup> and smart-material-based<sup>[80,81]</sup> actuation methods.

Due to its simplicity, large actuation stress and deformation, high energy efficiency, and low cost, pneumatic actuation is the most widely used method for the actuation of origami robots. In Figure 3a, Kim et al. report a pelican eel-inspired dual-morphing architecture that leverages a pneumatically driven system to achieve sequential transformations through origami unfolding and skin stretching.<sup>[68]</sup> This innovative design utilizes entirely stretchable origami units driven by pneumatic pressure to mimic the morphing principles of the pelican eel's stretchable and foldable frames. The dual-morphing response enables adaptive functionalities, including deployment-combined gripping, crawling, and extensive underwater locomotion, with an actuation force of up to 5 kg. By integrating the dual-morphing unit cells into conventional origami frames, the study demonstrates soft machines capable of extreme shape-morphing behaviors. Similarly, as shown in Figure 3b, Li et al. propose pneumatic-driven, origami-inspired artificial muscles that utilize a compressible skeleton, flexible skin, and a fluid medium to achieve multiaxial deformations, including contraction, bending, and torsion.<sup>[71]</sup> By using diverse materials and scalable fabrication methods, the authors can fabricate these artificial muscles at a low cost and in an efficient way. The artificial muscles demonstrate programmable motions with multiple degrees of freedom and controllable actuation rates. Under negative pressure, they contract over 90%, generate  $\approx 600$  kPa of stress, and deliver peak power densities above  $2 \text{ kW kg}^{-1}$ , which is reflected by a demonstration that a lightweight (less than 1 g) artificial muscle lifts a 22 kg car tire (Figure 3c). This high power-to-weight ratio and energy conversion efficiency ( $\approx 20\text{--}30\%$  in experimental setups) make pneumatic systems particularly advantageous for tasks requiring rapid shape transformation and large force outputs with relatively low energy costs. In a similar actuation approach, in Figure 3d, Zhang et al. introduce a pneumatic-driven, origami-based deformation module with a plug-and-play design that enables easy assembly. The module can achieve three fundamental deformation modes—bending, twisting, and contraction/extension—as well as four combined modes, resulting in seven distinct motion patterns.<sup>[72]</sup> Based on the Kresling origami pattern, the authors design a plug-and-play origami module where two new creases are added, and pneumatic pouches are placed at the crossing points between creases. By inflating or deflating these pouches, they break the original coupled deformation, achieving both independent contraction and bending. By assembling these origami modules, they built soft robots capable of performing complex, programmable tasks, which is demonstrated by an example where a three-module robotic arm grasps a cap and pours water (Figure 3e). This approach significantly surpasses conventional actuators and other origami-based designs in the diversity and decoupling of motion modes, empowering advanced capabilities in pneumatically driven soft robotics.

Cable-driven actuation is another widely used mechanism in robotics, known for its ability to offer high flexibility, low weight,

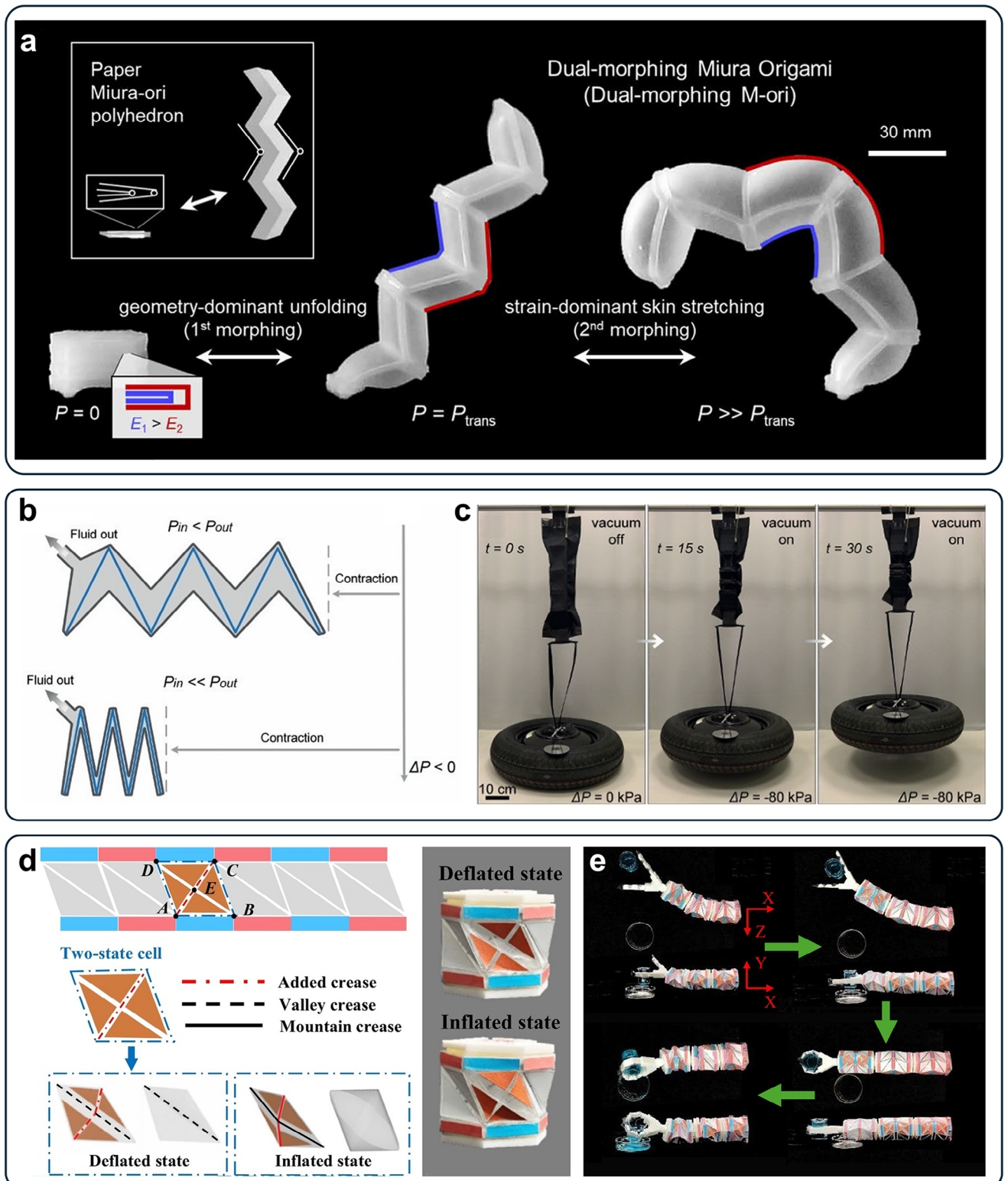


**Figure 3.** Pneumatic actuation method of origami robots. (a) Dual-Morphing Miura Origami: shape transformation under different pressure conditions.<sup>[68]</sup> (Copyright 2019, AAAS) (b) Working principle of origami-inspired artificial muscles.<sup>[71]</sup> (Copyright 2017, PNAS) (c) Lifting a car tire using origami-inspired artificial muscles.<sup>[71]</sup> (Copyright 2019, PNAS) (d) Improved design process of Kresling origami structures.<sup>[72]</sup> (Copyright 2023, Springer Nature) (e) Grasping and pouring a cup of water using origami mechanisms.<sup>[72]</sup> (Copyright 2023, Springer Nature).

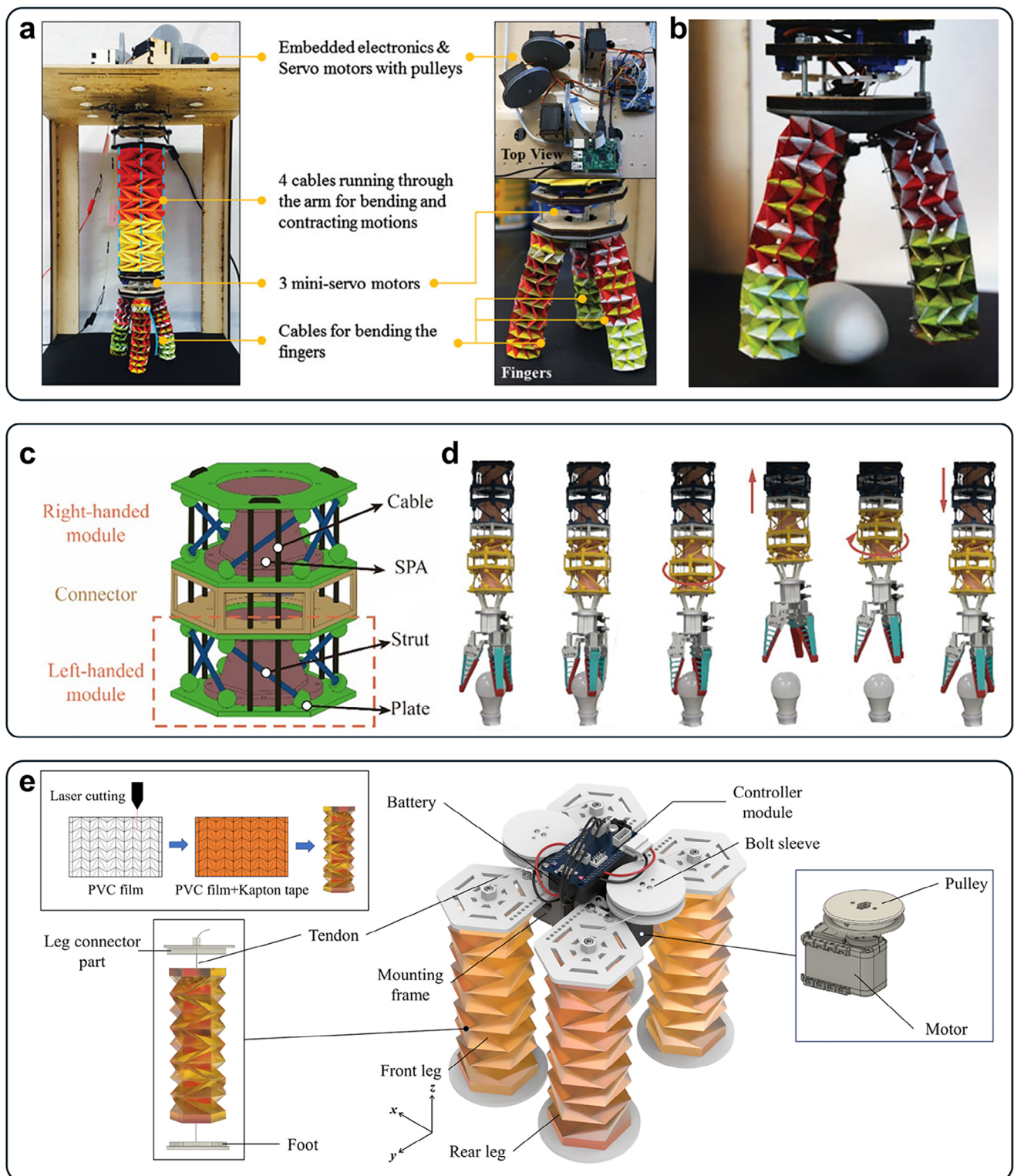


**Figure 4.** Cable-driven actuation method of origami robots. (a) Schematic diagram of a three-finger origami gripper system.<sup>[74]</sup> (Copyright 2017, Cambridge University Press) (b) Snapshot of the three-finger gripper holding an egg.<sup>[74]</sup> (Copyright 2017, Cambridge University Press) (c) Structural diagram of a two-level building block with the opposite chirality.<sup>[82]</sup> (Copyright 2025, John Wiley & Sons) (d) Snapshots of the continuum robot twisting a light bulb in one cycle.<sup>[82]</sup> (Copyright 2025, John Wiley & Sons) (e) Design, assembly, and actuation of an origami quadrupedal mobile robot.<sup>[76]</sup> (Copyright 2024, Elsevier).

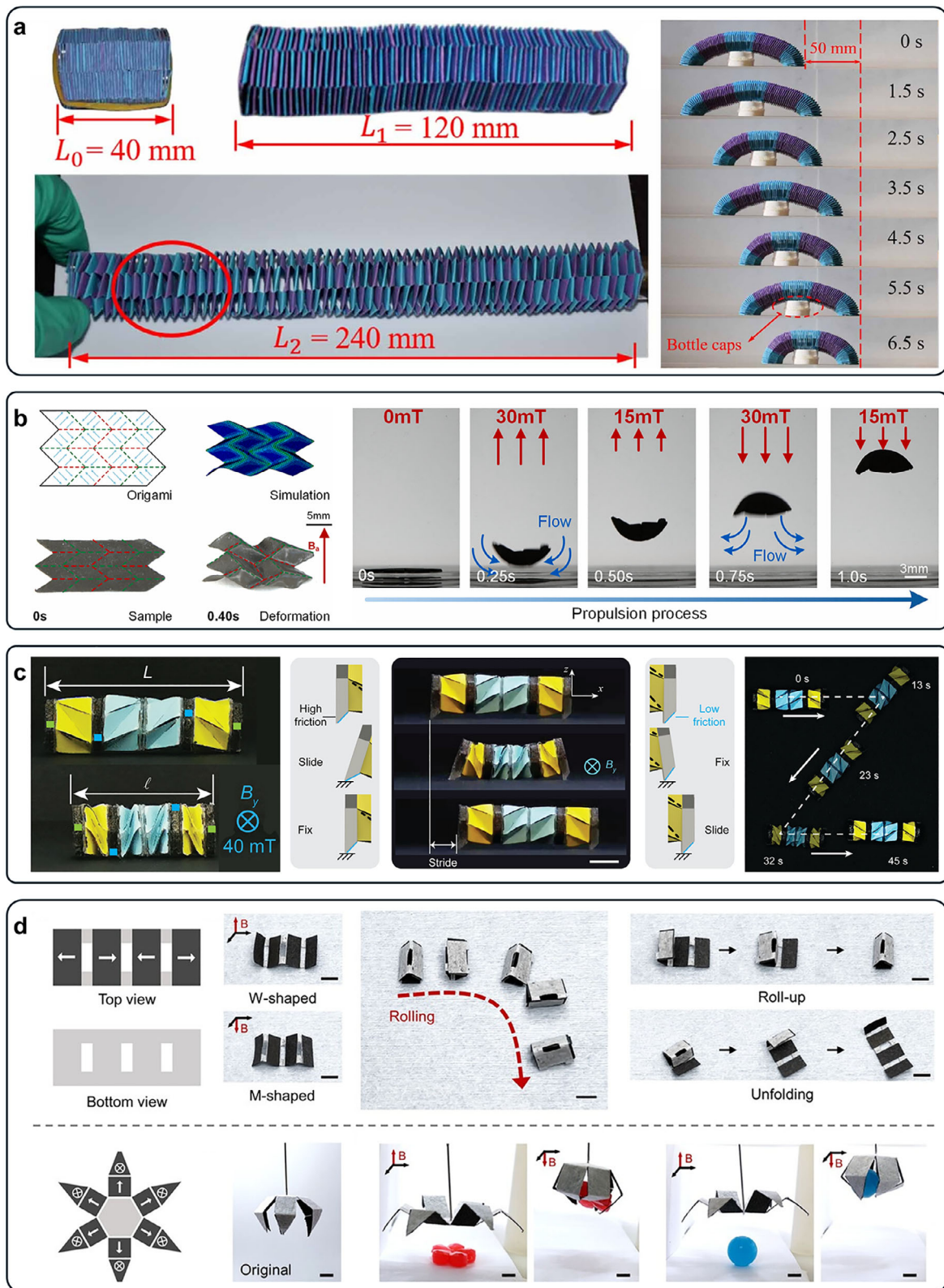


**Figure 5.** Magnetic actuation method of origami robots. (a) A soft origami robot mimicking worm-like motion actuated remotely through magnetic fields.<sup>[83]</sup> (Copyright 2023, IOP Publishing) (b) Magnetically actuated soft devices designed with origami principles, enabling customizable deformation behaviors.<sup>[84]</sup> (Copyright 2023, Elsevier) (c) Magnetic actuation and crawling motion of the Kresling origami robot.<sup>[39]</sup> (Copyright 2022, AAAS) (d) Magnetic actuation and locomotion performance of the Kresling crawler.<sup>[77]</sup> (Copyright 2024, John Wiley & Sons).

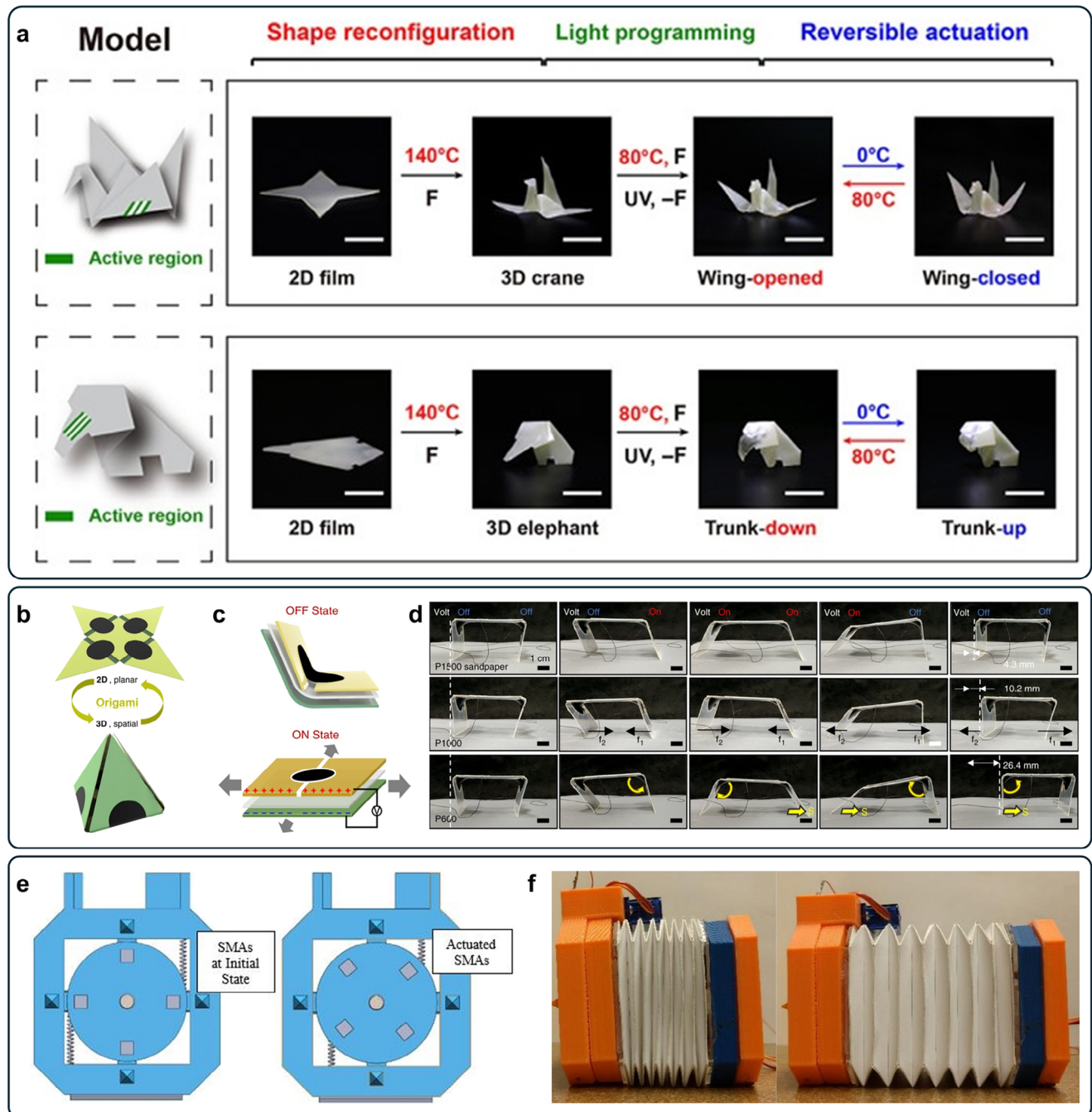


**Figure 6.** Smart-material-based actuation method of origami robots. (a) Fabrication and reversible actuation of the origami uni-bot.<sup>[104]</sup> (Copyright 2018, AAAS) (b) Origami-inspired soft robot schematic.<sup>[90]</sup> (Copyright 2022, Springer Nature) (c) Actuation principle and layered structure of the soft actuator with a VHB4910 dielectric layer.<sup>[90]</sup> (Copyright 2022, Springer Nature) (d) Analysis of soft robot behavior during crawling: actuator switching, force direction, and displacement direction.<sup>[90]</sup> (Copyright 2022, Springer Nature) (e) Schematic of the segmentation mechanism.<sup>[107]</sup> (Copyright 2017, ASME) (f) Photos of a crawling robot segment in the fully contracted state and fully expanded state.<sup>[107]</sup> (Copyright 2017, ASME).

and precise control over robotic movements. This technology utilizes cables or tendons to transmit forces and enable movement in various robotic structures, making it an attractive choice for applications requiring compact designs and intricate motions. Cable-driven systems are generally known for their high mechanical efficiency, especially when driven by servo motors with low

friction tendons. In recent years, researchers have explored the integration of cable-based actuation with origami patterns, leveraging the unique mechanical properties of foldable structures to create innovative robotic systems. For instance, as shown in Figure 4a, Jeong et al. developed a robotic manipulator with three fingers based on an origami twisted tower design and utilized

cable-driven actuation to achieve precise deformation for object manipulation.<sup>[74]</sup> The manipulator consists of a 10-layer twisted tower arm and three 11-layer twisted tower fingers, each actuated by cables connected to servo motors. Experimental evaluations demonstrate that the manipulator can successfully grasp and lift objects of various weights, sizes, and shapes, such as eggshells (Figure 4b), with a lifting capacity of 800 g per finger. This work highlights the potential of origami-inspired manipulators for delicate and adaptable robotic applications. As shown in Figure 4c, Wang et al. develop a rigid-flexible coupling module using cable-driven actuation, integrating a rigid parallel mechanism onto a soft origami base.<sup>[82]</sup> This modular unit enables three decoupled motions—contraction, bending, and twisting—via two oppositely chiral modules. The design retains origami's flexibility while boosting mechanical robustness, achieving an 180% increase in load-bearing and an 82.16% reduction in deformation error. A soft continuum robot built from this module (Figure 4d) demonstrated practical tasks like grasping and unscrewing a light bulb. Xu et al. propose a tendon-driven continuum robot (TDCR) using a telescoping assembly of super-elastic nitinol tubes as the backbone and a paper-based origami structure to guide the tendons, achieving lightweight and extensible deformation.<sup>[75]</sup> The robot operates through tendon-driven control to realize three degrees of freedom: yaw, pitch, and axial translation. The origami robot they designed has an extension ratio of more than 10 times and  $\pm 167$  degrees yaw/pitch angle with 21.9 g weight. Furthermore, as presented in Figure 4e, Kim et al. constructed a quadrupedal soft robot with tendon-driven Kresling-patterned origami cylinders as legs, achieving locomotion through folding and extending motions.<sup>[76]</sup> The robot utilizes the high axial stiffness of Kresling-patterned cylinders to provide a sufficient restoring force for movement, while the tendon-driven mechanism allows efficient actuation using only two motors without external devices. This design enables a bounding gait with a locomotion speed of  $47.51 \text{ mm s}^{-1}$ ,  $\approx 0.283$  body length per second. The origami structure not only enhances durability but also absorbs shocks, ensuring stable operation. This work highlights the potential of origami-inspired designs for efficient, durable, and adaptable locomotion in soft robots.

Magnetic actuation is a promising method for driving origami robots in a remote-controlled way due to its advantages, such as remote controllability, fast response, and high precision. This method relies on magnetic fields to generate forces and induce motion, enabling non-contact actuation that is particularly suitable for robots working in delicate or confined environments. Magnetic actuation is energy efficient in applications requiring intermittent control since no direct contact or onboard power source is needed. However, generating strong magnetic fields requires external coils or permanent magnets, which can lead to moderate energy demands. The efficiency of magnetic-to-mechanical energy conversion is usually low, but the remote and programmable nature often offsets this limitation in biomedical or confined space applications. Due to its ability to achieve complex, programmable deformations with minimal hardware requirements, magnetic actuation has been increasingly integrated with origami structures. In terms of response time, magnetic actuation typically provides sub-second responsiveness due to the instantaneous nature of magnetic field application. However, its force output is generally moderate and highly dependent on

the magnetic material properties and field strength, which limits its scalability for larger or high-load systems. As presented in Figure 5a, Jin et al. propose a worm-inspired origami robot using magnetic field-driven actuation and a novel paper-knitting technique.<sup>[83]</sup> Embedded magnetic discs in the backbone enabled precise, remote-controlled deformation, supporting versatile locomotion modes such as inchworm, Omega, and hybrid motions. The robot performed tasks like obstacle sweeping, wall climbing, and cargo delivery, achieving  $7.7 \text{ mm s}^{-1}$  transport speed in pipeline environments. In Figure 5b, Tang et al. design origami-based soft actuators with programmable deformation using magnetically responsive materials.<sup>[84]</sup> Their method enabled precise control over magnetic moment direction and deformation amplitude. Reconfigurable Miura folds and two-floor structures responded within 0.5 s to magnetic fields. A jellyfish-inspired actuator demonstrated efficient underwater propulsion via magnetic-induced lappet motions, converting field direction into lift and forward movement. Yuan et al. propose a magnetic spring robot (MSR) with a stretch-twist coupling origami spring skeleton actuated by a uniform magnetic field to generate diverse locomotion modes.<sup>[85]</sup> The robot utilizes a vertical folded origami structure (VFOS) with symmetric axial magnetization to achieve three distinct motion types: worm crawling, crab crawling, and rolling motion. This magnetic actuation method allows for efficient, untethered movement, making the MSR suitable for applications in environments such as in vivo diagnostics or therapeutic tools. Miyashita et al. introduce a miniature origami-based robot for clinical interventions, which is capable of performing versatile tasks such as wound patching, foreign body removal, drug delivery, and biodegradation.<sup>[78]</sup> Remotely controlled through external magnetic fields, the robot travels through the esophagus to the stomach, where it self-deploys and carries out targeted functions, such as patching wounds. As shown in Figure 5c, Ze et al. develop a magnetically actuated small-scale origami crawler using a four-unit Kresling assembly for effective in-plane contraction-based locomotion.<sup>[39]</sup> The Kresling origami pattern is carefully designed to avoid undesirable twists, enabling the crawler to achieve straight motion without lateral deviations. Magnetic actuation is employed to generate the necessary torque, which allows the crawler to contract for forward movement and provide instantaneous steering capabilities. As shown in Figure 5d, Chung et al. designed a biodegradable magnetic origami robot using magnetic paper that is both formable and recyclable.<sup>[77]</sup> The robot utilizes specific magnetization patterns and crease designs to achieve rapid deformation and movement under the influence of external magnetic fields. By applying a magnetic field, the origami actuator demonstrates dynamic and fast responses, such as wing flapping in a butterfly-shaped structure and rolling motions in a magnetic rolling robot. For magnetic actuation systems, performance degradation can occur due to the demagnetization of magnetic particles, mechanical fatigue of the structure, and potential delamination between magnetic and non-magnetic components over time. This degradation affects the precision and force output of the actuator, especially in applications requiring frequent and prolonged usage.

Smart materials are a type of materials that exhibit large deformation in response to external stimuli, such as temperature,<sup>[86–88]</sup> light,<sup>[89]</sup> or fields.<sup>[90–92]</sup> Smart materials offer high versatility, lightweight structures, and programmable functionalities,

which make them ideal for actuating origami robots in applications requiring lightweight, flexibility, and adaptability. Smart materials used to actuate origami robots mainly include shape memory polymers (SMPs),<sup>[93–96]</sup> shape memory alloys (SMAs),<sup>[97–99]</sup> dielectric elastomer actuators (DEAs),<sup>[90–92,100]</sup> and others.<sup>[77,79,101–103]</sup> As shown in Figure 6a, Jin et al. utilize crystalline SMPs (polyurethane) to develop a single-component polymeric robot termed the Origami Uni-bot (O-Unibot).<sup>[104]</sup> This innovation employs thermo-reversible bonds to create 3D-shaped structural support via a plasticity-based origami technique, while photo-reversible bonds enable spatially selective reversible shape memory actuation. The O-Unibot demonstrates the ability to perform complex soft robotic tasks, such as mimicking the movements of a crane and an elephant, highlighting its versatility. Unlike conventional multi-component robots that require intricate assembly of rigid and flexible materials, this approach successfully integrates structural support and actuation into a single component, addressing key challenges in soft robotics design. However, SMPs typically require thermal cycling with heating and cooling steps, leading to relatively low energy efficiency ( $\approx 1\text{--}3\%$ ) due to thermal losses.<sup>[105]</sup> The actuation time also tends to be slow (tens of seconds). In contrast, dielectric elastomer actuators exhibit higher actuation bandwidths and improved energy conversion efficiencies ( $\approx 10\text{--}15\%$ ), with low power consumption (typically under 1 W per unit) owing to their lightweight structure and high voltage, and low current operation.<sup>[106]</sup> As shown in Figure 6b, Sun et al. employ DEAs to develop programmable origami-inspired soft robots, addressing the response rate limitations inherent in SMP-based actuation.<sup>[90]</sup> By integrating multilayer DEA structures composed of pre-stretched VHB4910 elastomers as deformation layers and laser-cut PET films as flexible frames, they create a series of advanced soft robots capable of crawling and transforming between 2D and 3D configurations. One notable application, the crawling robot, demonstrates stable motion with enhanced speed on rough surfaces, achieving a maximum crawling speed of  $4.09 \text{ mm s}^{-1}$  on P600 sandpaper at a voltage of 5 kV and frequency of 0.29 Hz, as shown in Figure 6d. This performance highlights the effectiveness of DEA-driven systems in overcoming frictional challenges on varying terrains. While DEAs offer a significant improvement in actuation responsiveness and versatility, the approach is constrained by its limited load capacity and the requirement to position actuators at every hinge, restricting the application to simpler origami structures. As shown in Figure 6e, Angatkina et al. utilize SMA-based actuation to address the load capacity limitations of DEAs and develop a crawling robot inspired by the true metamerism of earthworms.<sup>[107]</sup> The robot's design employs modular segments constructed from bistable origami structures, which could extend and contract to enable crawling locomotion. These segments feature a docking system powered by SMA wire coils, allowing the robot to autonomously detach and reattach its segments using a directional magnetic arrangement. This modularity provides enhanced maneuverability and adaptability in various operational environments. As illustrated in Figure 6f, the bistability of the origami building blocks is effectively utilized to achieve power-efficient transitions between the fully contracted and expanded states of the robot segments, facilitating forward motion, and turning. This design demonstrates a significant advancement in robotic metamerism, en-

abling complex, multifunctional operations while maintaining high efficiency and scalability. Compared to magnetic actuation, smart material-based actuation, such as SMPs and SMAs, generally exhibits slower response times, often ranging from several seconds to minutes, due to heating and cooling requirements. DEAs, in contrast, offer faster response (typically in the range of tens to hundreds of milliseconds) with higher actuation bandwidth. In terms of force output, SMAs provide significantly higher actuation forces than DEAs or magnetic actuators, but at the cost of slower cycling and lower energy efficiency. Scalability is also a critical factor—while DEAs and SMPs are well-suited for miniaturized, lightweight systems, their performance diminishes with increased size due to voltage and thermal limitations. SMA-based systems are more scalable in terms of mechanical load but face control complexity and power requirements. For thermal-stimulated smart materials, thermal cycling leads to gradual fatigue, microstructural phase degradation, and mechanical wear, reducing actuation strain and force output over time. SMPs also exhibit plastic deformation or creep after prolonged exposure to heat. DEAs, on the other hand, are susceptible to dielectric breakdown and mechanical fatigue under high-voltage cycling. Although recent advancements have improved material resilience through new formulations and encapsulation strategies, the long-term reliability of smart-material-driven origami robots remains a key research area.

#### 4. 3D Printing Technologies for Fabricating Origami Robots

3D printing, also known as additive manufacturing, is an advanced manufacturing technology that fabricates 3D structures by incrementally depositing materials in a layer-by-layer manner. Its advantages, including design flexibility, precision, and compatibility with various materials, make it widely adopted for the fabrication of origami-inspired robots. Among the most commonly used 3D printing techniques for origami robots are FDM and DLP, which have shown particular success due to their ease of use, cost-effectiveness, and ability to create complex geometries. The mainstream 3D printing methods for manufacturing origami robots include: FDM, which extrudes melted thermoplastic filaments following prescribed patterns to create structures layer-by-layer (Figure 7a); DIW, an extrusion-based technique that prints shear-thinning inks capable of solidifying through various mechanisms such as evaporation, gelation, or phase change (Figure 7b); Polyjet printing, which jets photopolymer droplets onto a build platform and cures them using ultraviolet (UV) light to enable seamless multimaterial integration and functional structures (Figure 7c); DLP, which projects UV patterns onto liquid resins to trigger localized photopolymerization, resulting in highly intricate and refined 3D geometries (Figure 7d); and TPP, a nanoscale-resolution technology utilizing focused femtosecond laser pulses to induce localized polymerization within photosensitive resins, achieving microscale precision and multifunctionality (Figure 7e).

However, despite the broad applicability of these techniques, FDM and DLP are widely recognized as the two main 3D printing methods in origami robotics due to their established capabilities in producing robust and functional structures. FDM is favored for its affordability and versatility with materials, while

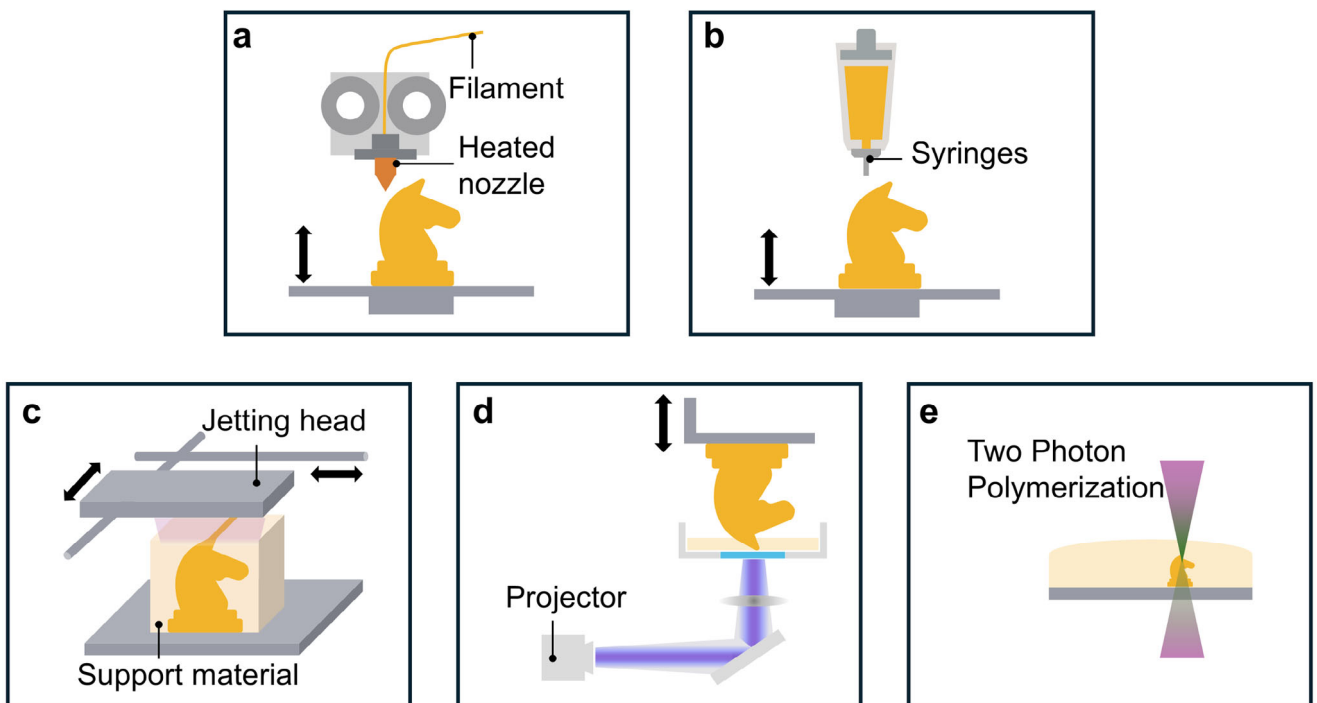


**Figure 7.** 3D printing technologies for fabricating origami structures. (a) Schematic illustration of FDM printing technology. (b) Schematic illustration of DIW printing technology. (c) Schematic illustration of Polyjet printing technology. (d) Schematic illustration of DLP printing technology. (e) Schematic illustration of TPP printing technology.

DLP stands out for its high resolution and ability to create intricate designs. These characteristics make them particularly suited for fabricating soft and rigid origami robots that require precise and reliable performance.

As illustrated in Figure 8, FDM has been widely adopted to fabricate origami structures and robots, due to its simplicity, cost-effectiveness, and compatibility with various engineering plastics. In addition to thermoplastic polymers, FDM has also been extended to include composites and bio-based materials, such as PLA with natural fibers or biodegradable thermoplastics, broadening the scope of material choices for environmentally conscious designs. As shown in Figure 8a-c, Faber et al. utilize FDM to fabricate a self-folding wing gripper, employing a printing method where rigid panels are naturally connected to flexible hinges.<sup>[108]</sup> This soft-rigid material integration is clearly visible in Figure 8b. The origami wing gripper incorporates spring elements into bioinspired origami structures, mimicking the bistable locking and rapid folding functionalities of the earwig's wing. As demonstrated in Figure 8c, the printed wing gripper is capable of quickly grasping and lifting heavy objects.

In Figure 8d, Xue et al. employs a multimaterial FDM 3D printer to fabricate a Yoshimura origami-based soft robot where rigid panels are strongly bonded with soft hinges through the encapsulation-based interface design strategy.<sup>[57]</sup> The soft-rigid coupled origami structure allows the robot to have higher load capacity and faster response speed compared with its purely soft counterparts. Origami robotic arms consisting of multiple units exhibit robust yet flexible structures (Figure 8e). In Figure 8f, the robotic arm demonstrates the capability to effortlessly grasp target objects. In Figure 8g, Xue et al. uses FDM-

based multmaterial 3D printing to create origami robotic grippers with rigid PLA panels and soft TPU hinges via a penetrating interface design.<sup>[30]</sup> Employing the Yoshimura pattern, they print foldable planar structures and assemble them into 3D tubes (Figure 8h). The grippers demonstrated over 90° bending and quick recovery (0.625 s) under cable-driven actuation. As shown in Figure 8i, they successfully grasped and placed a delicate dragon fruit without damage, highlighting their potential for gentle, adaptive manipulation in fields like the food industry. Melancon et al. use FDM to directly fabricate inflatable origami modules capable of multimodal deformations enabled by multi-stability.<sup>[109]</sup> This approach eliminates the need for folding assembly, which introduces overly complex post-processing steps. Figure 8e shows the bending deformation of an inflated module, highlighting its structural adaptability and functionality. As shown in Figure 8f, these modules are assembled into inflatable origami robotic arms, which can switch between various configurations to perform diverse tasks with simplified control mechanisms. In Figure 8j, Wang et al. employ FDM-based 4D printing with continuous fiber-reinforced composites to fabricate electrothermally controlled origami structures.<sup>[110]</sup> In this design, continuous carbon fibers (CCFs) are embedded into the hinge regions for Joule heating, enabling precise actuation, while fiber-reinforced regions form the rigid origami panels and non-reinforced areas serve as flexible creases. This integration not only ensures precise shape-shifting capabilities but also significantly enhances the structural stability and stiffness, with the reinforced rubbery state reaching up to 2.3 GPa—1000 times greater than that of pure SMP. As shown in Figure 8k, the resulting origami-based grippers exhibit programmable

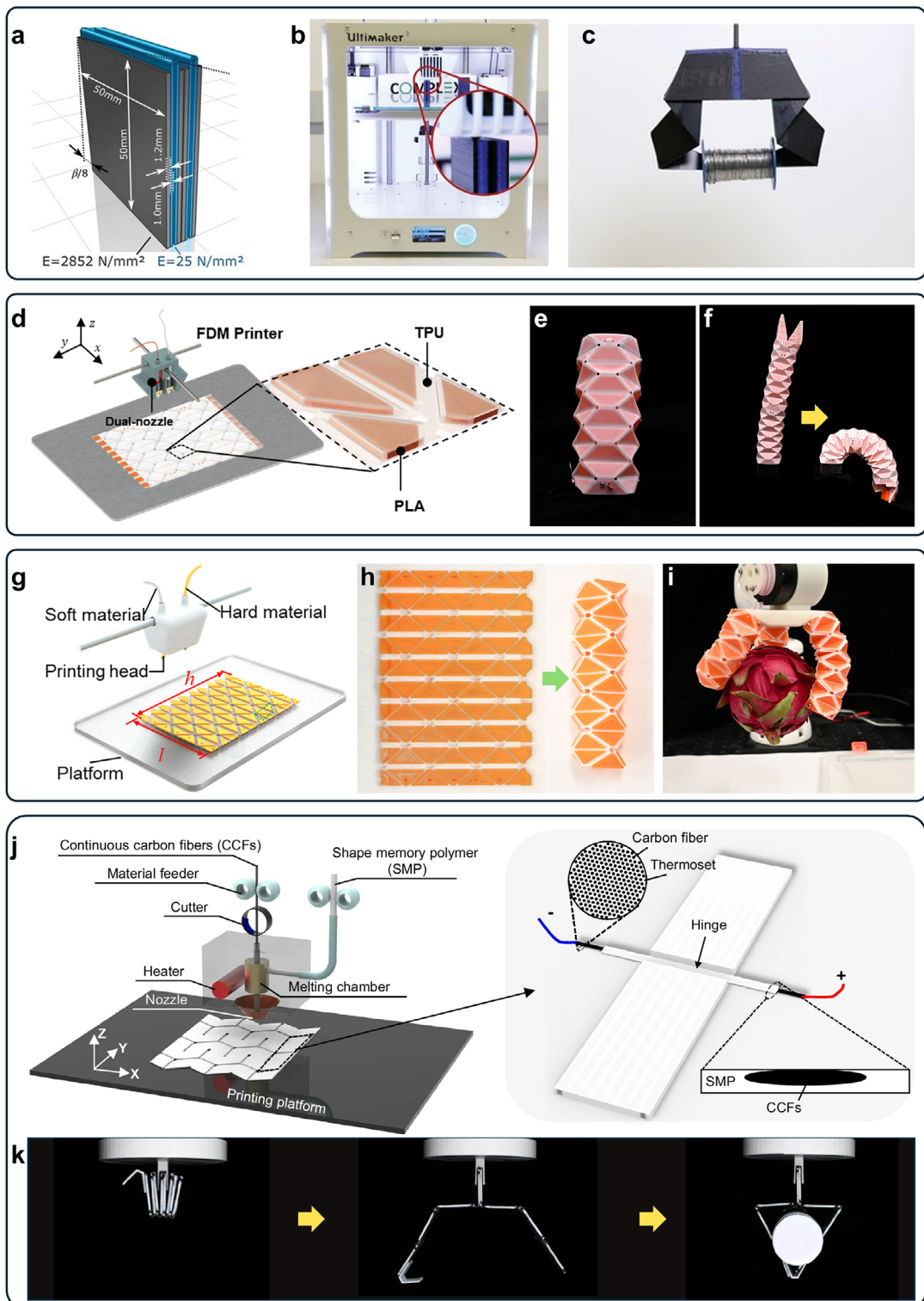


**Figure 8.** Origami robot fabricated using FDM 3D printing. (a) Geometry and material properties.<sup>[108]</sup> (Copyright 2018, AAAS) (b) FDM printing in the folded, upright state.<sup>[108]</sup> (Copyright 2018, AAAS) (c) Spring origami gripper is in a closed state.<sup>[108]</sup> (Copyright 2018, AAAS) (d) Multimaterial FDM printing of PLA panels with TPU hinges for 2D crease patterns.<sup>[57]</sup> (Copyright 2024, IOP Publishing) (e) The origami robot in the up-right configuration.<sup>[57]</sup> (Copyright 2024, IOP Publishing) (f) Grasping process snapshots.<sup>[57]</sup> (Copyright 2024, IOP Publishing) (g) Illustration of using an FDM multimaterial 3D printer to fabricate a multimaterial origami pattern.<sup>[30]</sup> (Copyright 2025, Mary Ann Liebert) (h) Snapshots of the process that transforms a flat crease origami pattern into a 3D origami structure.<sup>[30]</sup> (i) Grasping and placing a dragon fruit.<sup>[30]</sup> (Copyright 2025, Mary Ann Liebert) (j) 3D printing of CCF-SMP PCEO composite and electrothermal hinge with joule heating CCF integration.<sup>[110]</sup> (Copyright 2024, Springer Nature) (k) Snapshots of the robotic gripper grasping a solid adhesive rod.<sup>[110]</sup> (Copyright 2024, Springer Nature).

shape-changing behavior, enabling high precision, responsiveness, and adaptability. These grippers demonstrate remarkable control, effectively grasping and manipulating target objects with diverse configurations.

However, it is important to note that the relatively low resolution of FDM printing can negatively impact the mechanical performance and folding precision of the resulting origami structures. The layer-by-layer deposition and larger nozzle diameters associated with FDM may lead to surface roughness, dimensional inaccuracies, and imperfect hinge formation. These limitations can reduce the sharpness of fold lines, introduce residual stresses at bending regions, and impair the repeatability and reliability of shape transformations. Consequently, although FDM offers cost-effectiveness and ease of use, it may not be the optimal choice for applications requiring high-fidelity folding or delicate mechanical responses if high resolution is required. In contrast, higher-resolution techniques such as DIW, DLP, or TPP can produce finer features and more accurate creases, which are essential for precise shape morphing and mechanical performance in complex origami systems.

As illustrated in **Figure 9**, DIW is another extrusion-based 3D printing technology that fabricates 3D structures by extruding shear-thinning inks, including colloidal suspensions, colloidal gels, polymer melts, dilute colloidal fluids, and others.<sup>[111,112]</sup> These inks solidify either through liquid evaporation, gelation, or a temperature- or solvent-induced phase change. Compared with FDM, DIW allows users to have a higher degree of freedom to customize printing materials and print structures with functional materials. As shown in **Figure 9a**, Kim et al. utilize DIW to print soft origami structures with ferromagnetic domains, where the magnetized regions form the origami panels, while the non-magnetized extruded material serves as hinges.<sup>[48]</sup> The actuation mechanism is presented in **Figure 9b**. **Figure 9c** shows the fabricated origami structure undergoing shape transformation under an applied magnetic field. This approach enables untethered, fast-transforming soft actuators and robots with programmable shape morphing and reconfigurability. As shown in **Figure 9d**, Liu et al. report ceramic 4D printing by employing DIW to fabricate 2D Miura origami patterns with elastomer-derived ceramics.<sup>[113]</sup> In the DIW process, shear-thinning ceramic inks are extruded through a nozzle, allowing precise deposition of material onto a substrate to create the desired pattern. Upon mechanical loading, these 2D patterns fold into 3D geometries (**Figure 9e**). Further debinding and sintering processes are then applied, removing the polymeric binders, and densifying the ceramic material, resulting in pure 3D ceramic structures with excellent mechanical properties. In order to realize multimaterial DIW printing with fast switching speed, as shown in **Figure 9f**, Skylar–Scott et al. report multimaterial multinozzle 3D (MM3D) printing where the printing heads exploit the diode-like behavior that arises when multiple viscoelastic materials converge at a junction to enable seamless and high-frequency switching.<sup>[114]</sup> The process involves depositing hard and soft materials alternately, with precise control over material placement, to form foldable Miura–Origami structures. **Figure 9g** shows a flexible hinge connecting two hard panels, while **Figure 9f** presents the complete foldable Miura–Origami structures, where the hard panels and soft hinges are seamlessly integrated, demonstrating the effectiveness of the MM3D printing method.

As illustrated in **Figure 10**, different from extrusion-based 3D printing technology, Polyjet technology creates 3D objects by jetting photopolymer droplets onto a build platform and curing them with UV light. Polyjet allows for the fabrication of intricate, functional, and multimaterial structures with seamless integration, and thus has been applied to fabricate functional origami structures. As shown in **Figure 10a**, Ge et al. propose printed active composite materials (PACs, **Figure 10b**) using Polyjet 3D printing to create complex origami-inspired structures with shape memory behaviors.<sup>[86]</sup> The process involves designing the fiber and matrix architecture in a CAD file and is followed by printing multiple layers to form a laminate with thermomechanical properties. This approach enables the fabrication of structures capable of bending, twisting, folding, and coiling, with the ability to return to their original shape upon reheating, as demonstrated in **Figure 10c**. The combination of shape memory fibers and elastomeric matrices imbues the structure with dynamic, programmable deformation, allowing for applications such as self-folding devices. As shown in **Figure 10d**, Ge et al. report 4D printed active origami structures by using Polyjet to print origami patterns with active composite hinges where shape memory fibers are embedded in the elastomeric matrix.<sup>[87]</sup> As shown in **Figure 10e**, a 2D triangle evolves into a 3D origami crane after the thermomechanical programming process. As shown in **Figure 10f,g**, Yuan et al. utilize Polyjet technology to fabricate more intricate self-folding origami structures, such as self-folding Miura-ori and self-folding crane, by applying specialized designs to the active composite hinges.<sup>[88]</sup> These enhancements demonstrate the potential of Polyjet-based PACs for advanced applications requiring precise and complex shape transformations. In **Figure 10h**, Mao et al. propose a novel method to create sequentially self-folding structures using Polyjet 3D printing to fabricate hinges with digital SMPs.<sup>[93]</sup> By mixing two base materials at specific ratios, they achieved programmable thermomechanical properties, enabling self-folding at controlled speeds under a uniform temperature field. This approach eliminates the need for complex localized heating systems and allows for precise design and fabrication of complex self-folding and self-locking structures. As shown in **Figure 10i**, a 4D-printed origami box with sequential folding is realized by assigning SMPs with different glass transition temperatures to specific hinges. As shown in **Figure 10j**, Lee et al. design an underactuated robotic gripper, TWISTER Hand, inspired by the twisted tower origami principle.<sup>[115]</sup> Fabricated using Polyjet 3D printing, the gripper achieves precise structure and functionality, as detailed in **Figure 10k**, which presents its grasping and releasing actions, demonstrating flexible grasping capabilities. The use of Polyjet 3D printing enables precise fabrication, efficient force transmission, and a lightweight design, making TWISTER Hand suitable for handling delicate objects in robotic applications.

**Figure 11** illustrates the DLP 3D printing technology that fabricates 3D structures by projecting 2D ultraviolet (UV) patterns onto the surface of polymer resin to trigger localized photopolymerization converting liquid resin to 3D solids.<sup>[116]</sup> DLP can print most photopolymerizable resins, and recent developments in DLP have introduced the use of non-photopolymerizable materials such as ceramics and metal composites, expanding its material palette to include functional, high-performance materials.

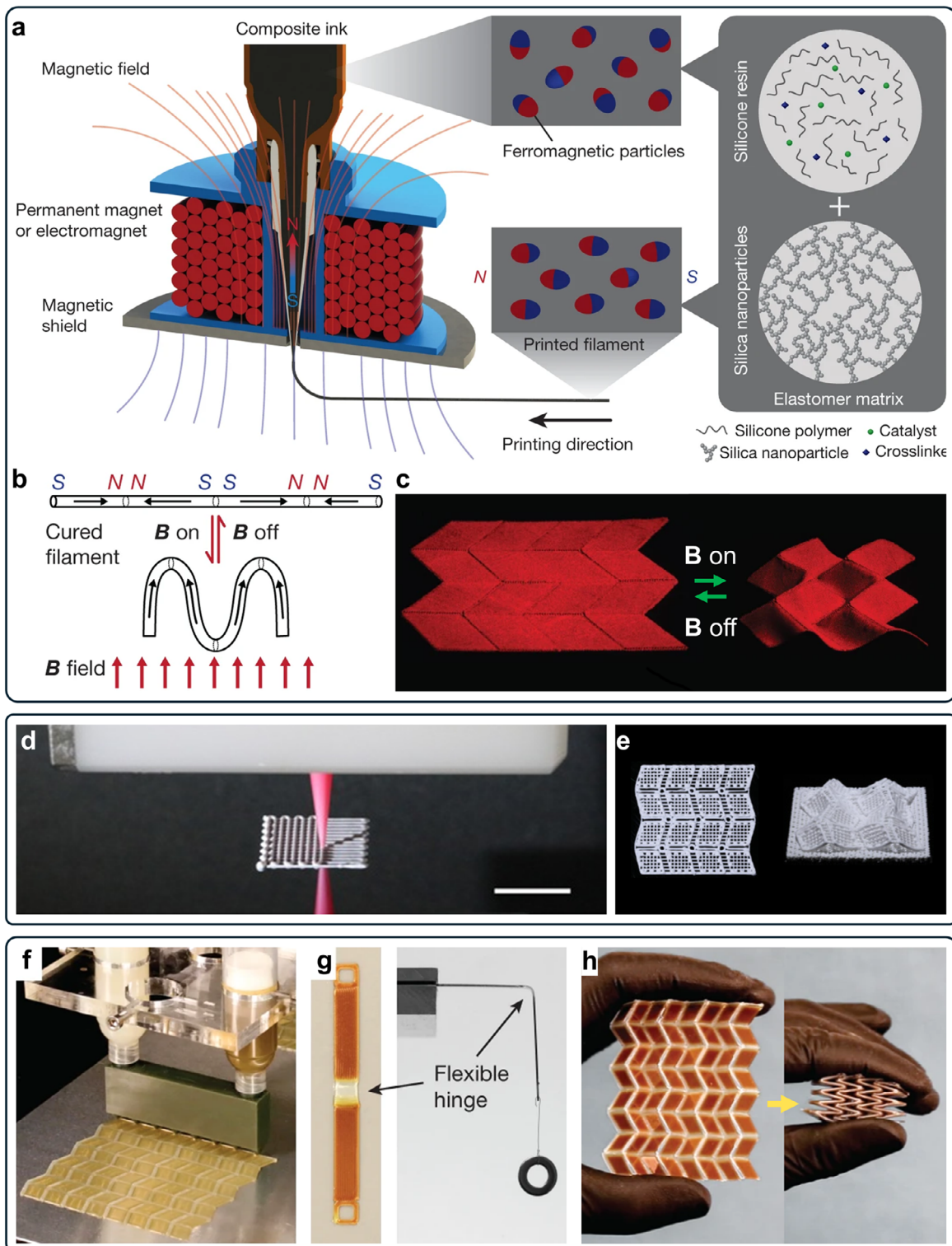


**Figure 9.** Origami robot fabricated using DIW 3D printing. (a) Schematics of the printing process and material composition: ferromagnetic particles in composite ink reoriented by a magnetic field near the dispensing nozzle.<sup>[48]</sup> (Copyright 2018, Springer Nature) (b) Magnetic actuation simulation of finite-element model.<sup>[48]</sup> (Copyright 2018, Springer Nature) (c) Experimental results of Miura-ori fold with alternating oblique ferromagnetic patterns.<sup>[48]</sup> (Copyright 2018, Springer Nature) (d) Optical image of DIW.<sup>[113]</sup> (Copyright 2018, IOP Publishing) (e) 4D-printed EDCs with Miura-ori design.<sup>[113]</sup> (Copyright 2018, IOP Publishing) (f) MM3D printing of a Miura pattern with an 8 × 1 two-material printhead.<sup>[114]</sup> (Copyright 2019, Springer Nature) (g) Patterned bending of stiff cantilevers (orange) and a flexible hinge (grey).<sup>[114]</sup> (Copyright 2019, Springer Nature) (h) Folding behavior of an 8 × 8 Miura pattern.<sup>[114]</sup> (Copyright 2019, Springer Nature).

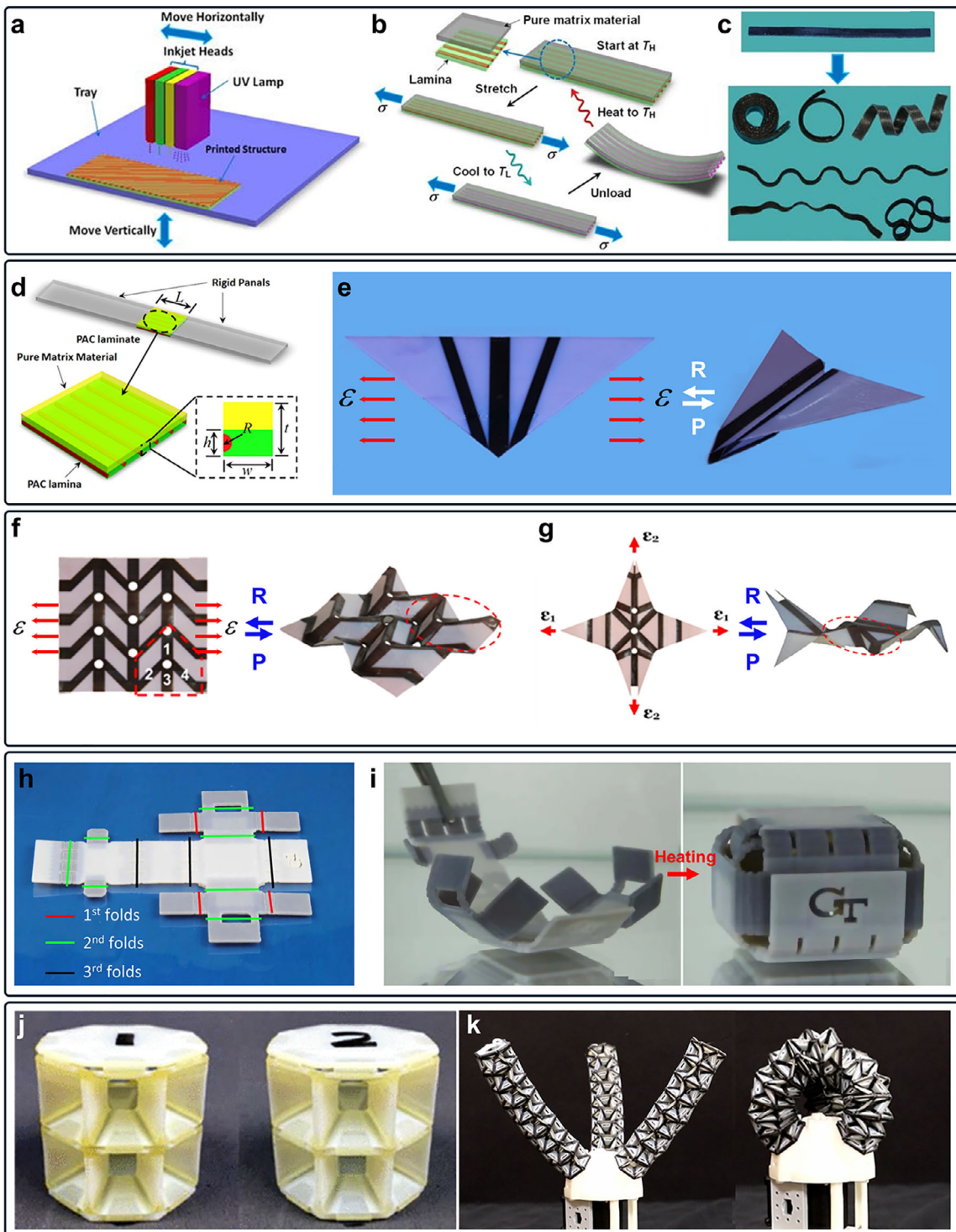


**Figure 10.** Origami robot fabricated using Polyjet 3D printing. (a) Schematic of the printed active composite printing process.<sup>[86]</sup> (Copyright 2013, AIP Publishing) (b) PAC lamina schematic: a two-layer laminate combining fiber-oriented lamina and pure matrix material, processed through heating, stretching, cooling, and release.<sup>[86]</sup> (Copyright 2013, AIP Publishing) (c) Original strip and outcomes under varying fiber architectures.<sup>[86]</sup> (Copyright 2013, AIP Publishing) (d) Schematics of a PAC hinge and the thermomechanical programming steps.<sup>[87]</sup> (Copyright 2014, IOP Publishing) (e) A hinged triangular sheet folding into an origami airplane.<sup>[87]</sup> (Copyright 2014, IOP Publishing) (f) Self-Folding Miura-ori.<sup>[88]</sup> (Copyright 2017, Springer Nature) (g) Self-Folding crane.<sup>[88]</sup> (Copyright 2017, Springer Nature) (h) Programmed 3D-printed sheet with varied hinge materials.<sup>[93]</sup> (Copyright 2015, Springer Nature) (i) Heating induces folding into a self-locking box.<sup>[93]</sup> (Copyright 2015, Springer Nature) (j) 3D Printed TWISTER structure with TangoPlus material.<sup>[115]</sup> (Copyright 2020, IEEE) (k) Underactuated cable-driven robotic gripper with three compliant fingers: fully open (left) and closed (right).<sup>[115]</sup> (Copyright 2020, IEEE).

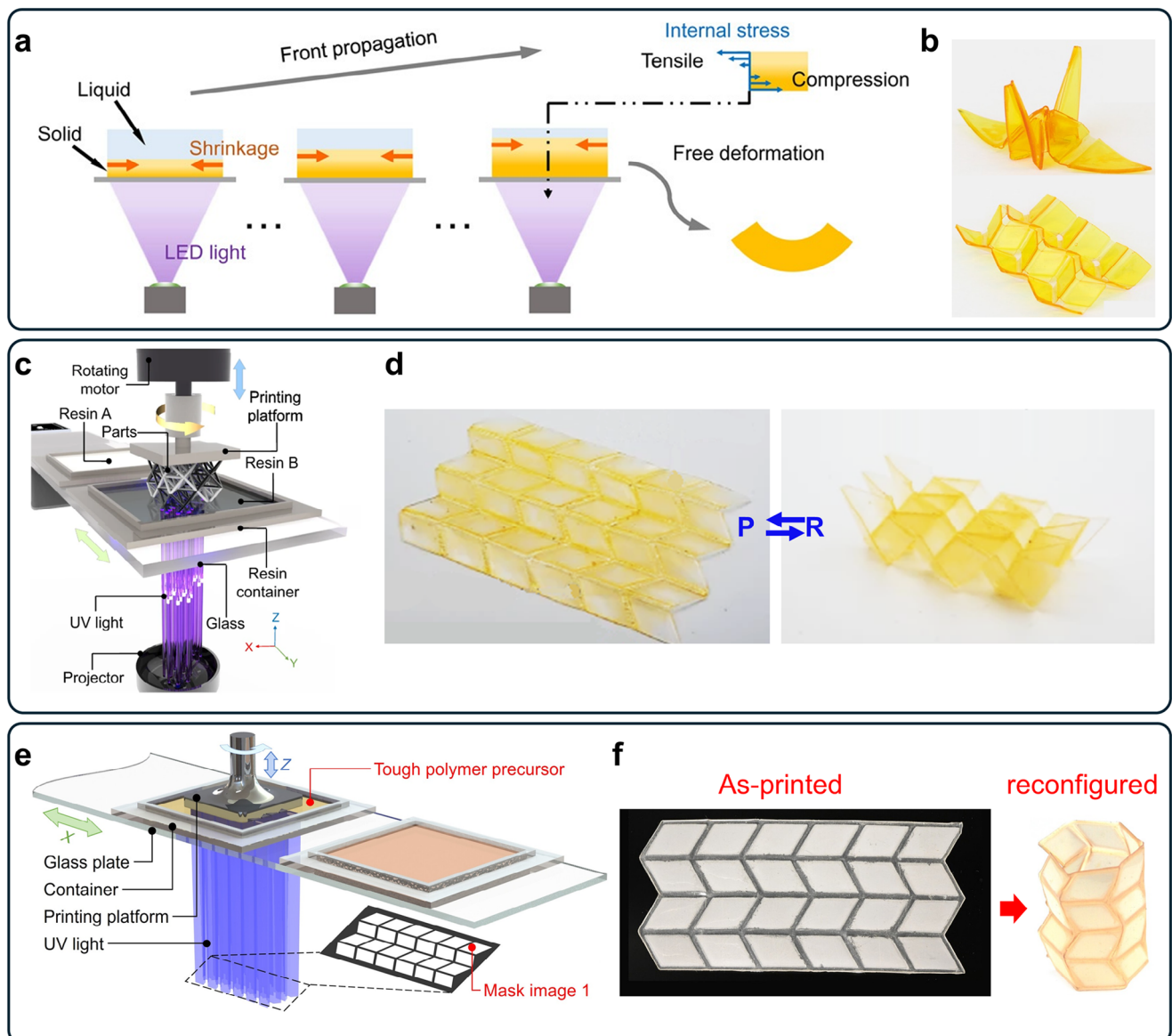


**Figure 11.** Origami robot fabricated using DLP 3D printing. (a) Volume shrinkage-induced bending: sequential shrinkage during FPP of a polymer sheet generates internal stress, driving the sheet to bend.<sup>[117]</sup> (Copyright 2017, AAAS) (b) Fabrication of Miura and crane structures via two-side illuminations.<sup>[117]</sup> (Copyright 2017, AAAS) (c) Illustration of the CM 3D printing system.<sup>[118]</sup> (Copyright 2022, Springer Nature) (d) Miura-origami sheet with hard polymer panels and SM polymer hinges.<sup>[118]</sup> (Copyright 2022, Springer Nature) (e) Schematic of multimaterial printing reconfigurable origami.<sup>[119]</sup> (Copyright 2024, AAAS) (f) Demonstration of shape-memory behaviors in reconfigurable origami.<sup>[119]</sup> (Copyright 2024, AAAS).

Compared with FDM, DIW, and Polyjet, DLP is capable of creating 3D structures with intricate geometries and refined details. Thus, DLP is also widely adopted to fabricate origami structures. As presented in Figure 11a, Zhao et al. introduce a method for fabricating 3D origami structures using a frontal photopolymerization (FPP) approach, similar to DLP 3D printing, leveraging photopolymerization-induced volume shrinkage to achieve spontaneous shape morphing.<sup>[117]</sup> Light projected through a transparent substrate cures a liquid resin layer by layer, with the addition of photoabsorbers creating a gradient in curing intensity. This nonuniform curing induces internal stress gradients, driving the material to bend toward newly cured regions upon re-

lease from the substrate. As shown in Figure 11b, this process enables the creation of complex 3D origami shapes (Miura structures and Crane structures) without external stimuli, offering a simplified and efficient alternative for fabricating intricate structures. Origami structures with higher mechanical performance and more functionalities can be fabricated by DLP-based multimaterial 3D printing.

In Figure 11c, Cheng et al. apply centrifugal multimaterial DLP 3D printing to create a shape memory Miura origami structure where the panels are printed with hard polymer and connected with shape memory hinges.<sup>[118]</sup> The printed 2D origami sheet can be folded to and fixed at the 3D shape which later turns

to the 2D sheet upon heating. As shown in Figure 11e, Li et al. propose reconfigurable 4D-printed structures using mechanically robust covalent adaptable network shape memory polymers (MRC-SMPs) fabricated through DLP 3D printing.<sup>[119]</sup> As shown in Figure 11f, the high-resolution printing process enables the creation of complex SMP structures that can be reconfigured into multiple permanent shapes under large deformations. The MRC-SMPs exhibit exceptional thermomechanical properties, including high deformability (>1400%), a high glass transition temperature (75 °C), and excellent weldability, allowing separate parts to merge seamlessly after heat treatment. This innovation supports applications such as programmable hinges, reconfigurable lattice-based robotic grippers, and origami-inspired devices for versatile shape-morphing functions.

As illustrated in Figure 12, TPP 3D printing technology employs focused femtosecond laser pulses to selectively induce localized polymerization within a photosensitive resin.<sup>[120,121]</sup> It is notable for overcoming the diffraction limit, enabling the fabrication of features with exceptional resolution. This technology excels in producing intricate 3D micro/nanostructures and offers significant advantages in terms of printing flexibility and spatial resolution, making it highly effective for the fabrication of precise microstructures.<sup>[122]</sup> As shown in Figure 12a, Ceylan et al. employ TPP to fabricate a structure with dual helical configurations, designed for cargo loading and responsive swimming under the influence of a rotating magnetic field.<sup>[123]</sup> These microswimmers are 3D printed from a magnetic precursor mixture containing gelatin methacryloyl (GelMA) and biofunctionalized superparamagnetic Fe<sub>3</sub>O<sub>4</sub> nanoparticles, enabling precise control over both the structural design and functional properties. Figure 12b,c demonstrate the detailed morphology of the microswimmers, highlighting the homogeneous embedding of magnetic nanoparticles, which facilitates efficient magnetic actuation and environmental responsiveness. This work underscores the potential of TPP-fabricated microswimmers for advanced therapeutic and diagnostic applications in physiologically complex environments. Drawing inspiration from modular robots and Lego-like blocks, as illustrated in Figure 12d, Huang et al. introduce a programmable design approach for the direct construction of 3D reconfigurable microstructures, enabling complex shape transformations.<sup>[124]</sup> These robots are achieved using stimuli-responsive hydrogel micro-blocks fabricated through TPP-based 4D printing. By temporally and spatially controlling the direct writing process, varying crosslinked polymer networks are formed. In response to environmental pH changes, the origami structures function as actuators, transitioning between open and closed positions. The transformer, capable of multiple distinct deformations, can morph from a race car to a human-like robot. As illustrated in Figure 12e, the 4D micro-building blocks exhibit high precision, programmability, and reconfigurable properties, significantly broadening the design space for microfabricated devices. As illustrated in Figure 12f, Jin et al. introduce an advanced strategy for 4D microprinting by utilizing TPP-based laser writing to fabricate reconfigurable compound micromachines with exceptional mechanical properties.<sup>[125]</sup> This approach involves the creation of shape-morphing micromachines using phototunable, stimulus-responsive hydrogels. By controlling parameters such as the femtosecond laser exposure dose, crosslinking densities, and other factors like stiffness and swelling/shrinking be-

havior, the material properties can be finely tuned to achieve the desired performance. Finite element methods are employed to predict the characterization and shape-changing behaviors of the micromachines. Unlike bilayered structures, this method allows for extensive shape transformations. Figure 12g showcases various reconfigurable micromachines, including microcages, microstents, and microumbrellas, demonstrating their ability to undergo rapid, precise, uniaxial, and biaxial contraction, reversible shape changes, and articulated bar folding.

**Table 1** provides a comparative summary of the main 3D printing techniques for origami robot fabrication. FDM stands out for its simplicity, low cost, and wide material compatibility, but it suffers from relatively low resolution and poor surface finish, which may limit applications requiring high folding precision. DIW offers greater material customizability and enables multimaterial integration, especially useful for functional inks or stimuli-responsive structures; however, it typically has lower mechanical strength and slower printing speed. Polyjet and DLP are advantageous for high-resolution, multimaterial fabrication with smooth surfaces, though they require expensive photopolymer resins and equipment, limiting their scalability. TPP, with its ultrahigh resolution, is ideal for micro- and nanoscale origami systems, but its slow throughput and limited printable volume currently constrain large-scale robotic applications.

## 5. Conclusion and Perspectives

In the above sections, we present a comprehensive review on the recent advancements of origami robots in terms of crease patterns for 3D origami structures, actuation methods for driving origami robots, and 3D printing methods for fabricating origami robots. In the past decade, numerous 3D printed origami robots have been developed for applications such as grasping objects with different shapes, locomotion, and biomedical operations on a micrometer scale. However, the adoption of 3D printed origami robots to broader applications is hindered in the following aspects: 3D printing capability, design methods for origami patterns, and breakthrough applications.

### 5.1. 3D Printing Capabilities

FDM and DLP are the two 3D printing techniques used to fabricate soft-hard coupled origami robots. However, both techniques have limitations. FDM-based multimaterial 3D printing technique fabricates soft-hard coupled origami robots with industrial polymers (i.e., TPU, PLA, etc.), which have robust mechanical performance. However, forming robust interfacial bonding between the soft and hard polymers remains a key challenge. Despite the recent works reporting the encapsulation method to a strong bond between soft hinges and hard panels,<sup>[46,47,57]</sup> this method sacrifices the printing efficiency as the soft skins are required to be printed to encapsulate the hard panels. Therefore, new methods are demanded to achieve strong interfacial bonds between soft and hard materials without sacrificing the printing time. On the other hand, DLP-based multimaterial 3D printing technique is capable of forming a strong interface between soft and hard materials due to the covalent bonds between

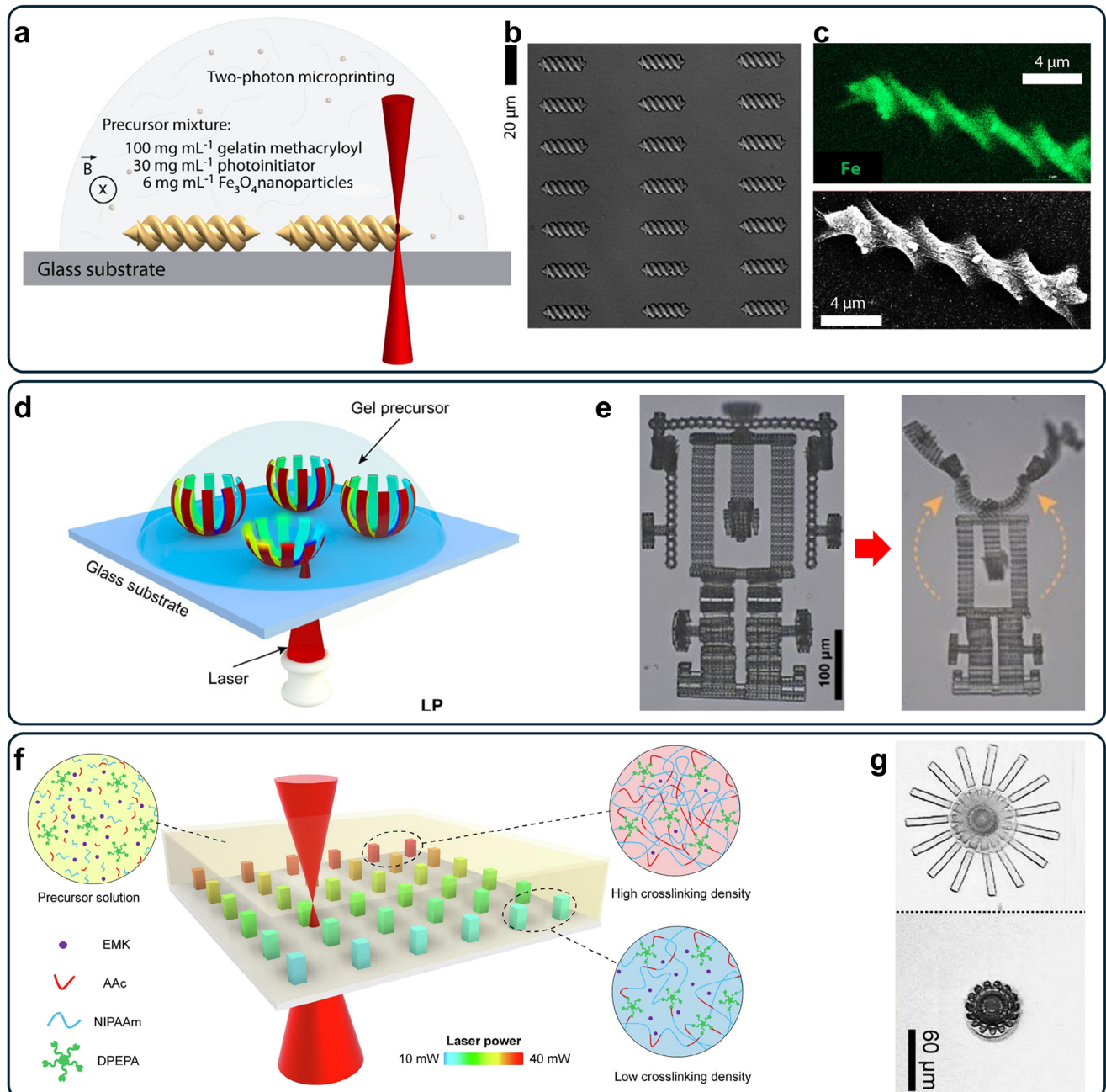


**Figure 12.** Origami robot fabricated using TPP 3D printing. (a) 3D fabrication of micro-swimmers using two-photon polymerization with continuous magnetic field alignment of nanoparticles.<sup>[123]</sup> (Copyright 2019, ACS Publications) (b) Optical microscope DIC image of a micro-swimmer array.<sup>[123]</sup> (Copyright 2019, ACS Publications) (c) Energy-dispersive X-ray spectroscopy mapping confirms the uniform embedding of iron oxide magnetic nanoparticles within the micro swimmer body.<sup>[123]</sup> (Copyright 2019, ACS Publications) (d) Schematic of the printing process in a DLW system.<sup>[124]</sup> (Copyright 2020, AAAS) (e) Sequential optical images of the 3D shape morphing from a race car to a humanoid robot.<sup>[124]</sup> (Copyright 2020, AAAS) (f) Schematic of the 4D-DLW process, where cuboid microstructures with increasing crosslinking density are printed from a hydrogel precursor by increasing laser power.<sup>[125]</sup> (Copyright 2020, Elsevier) (g) 3D-to-3D Reconfigurable Micro-Umbrella Demonstration.<sup>[125]</sup> (Copyright 2020, Elsevier).

them generated from the photopolymerization process. Yet, compared with these industrial materials for FDM, the photocurable polymers for DLP are pale in terms of mechanical robustness and environmental stability. Therefore, better photocurable polymers are desired for DLP printing origami robots. To address these material limitations, the development of new photocurable

resins with enhanced mechanical strength, biocompatibility, and thermal stability is critical. Key factors in developing new 3D printing materials include improving interfacial adhesion properties, enabling programmable stiffness, ensuring printability under multi-material conditions, and achieving durability under cyclic deformation. Additionally, hybrid materials that combine

**Table 1.** Comparison of Different 3D Printing Technologies for Origami Robot Fabrication.

Property	3D Printing Technologies				
	FDM	DIW	Polyjet	DLP	TPP
Material Types	Thermoplastics (PLA, ABS, TPU)	Shear-thinning inks (polymer melts, colloidal suspensions, etc.)	Photopolymers, multi-materials	Photopolymers (liquid resins)	Photosensitive resins
Printing Resolution	Moderate (0.1–0.4 mm)	Moderate (0.1–0.3 mm)	High (0.02–0.1 mm)	Very high (0.025 mm)	Extremely high (nanoscale)
Speed	Moderate	Moderate	High	High	Low
Material Compatibility	Wide range (plastics, composites)	High customization potential	Limited to photopolymer materials	Limited to photopolymer materials	Limited to photosensitive resins
Cost	Low	Moderate	High	Moderate to High	High
Applications	Low-cost, general-purpose printing	Soft actuators, multimaterial structures	Functional multimaterial structures	High-resolution origami robots	Microscale precision applications, high-functionality robots

nanofillers or dynamic covalent chemistry may offer pathways to tunable performance and longer-term reliability.

## 5.2. Design for Origami Robots

Modeling and designing the kinematic behaviors of an origami robot requires to build the relations between the flattened crease pattern and the geometry as well as the kinematics of folded 3D origami structures. The entire modeling process involves a large number of geometric parameters and complicated calculations of the matrix and is an expensive computational process. To model and design the dynamic behaviors of an origami robot, the mechanical properties of the materials used to build the origami robot need to be integrated into the complex matrix computation, which further burdens the modeling process. In addition, enriching the functionality of designed origami robots, more than one crease pattern would be used to build the origami robots, which makes modeling become more challenging. The expensive modeling cost is another reason that hinders the origami robots from engineering applications. With the boom in artificial intelligence,<sup>[126–128]</sup> a machine learning-based design approach might be a solution to make the design and modeling of origami robots easier.<sup>[129,130]</sup> Machine learning can be applied to accelerate the inverse design process by learning mappings between crease patterns and functional outcomes. It can also be employed to optimize crease configurations for specific tasks. By reducing the reliance on iterative numerical simulations and enabling rapid prediction of structural behavior,<sup>[131,132]</sup> ML approaches significantly lower computational costs and enable real-time design feedback, especially for multi-functional or reconfigurable origami robots.

## 5.3. Breakthrough Application

In this review paper, many frontier research outcomes on origami robots have been introduced and analyzed. Researchers have reported advanced approaches for designing, manufacturing, and actuating origami robots. However, the applications demonstrated in most of these works are still at the conceptual level.

Compared with traditional industrial robots or even frontier soft robots, origami robots are barely used in real application scenarios. Therefore, researchers need to further explore the potential of origami robots and find the application scenarios where the advantages of origami robots (i.e., high flexibility, large contraction ratio, high energy absorption, the capability of modular design and assembly) match well. Some works<sup>[133–135,67]</sup> show the potential of microscale origami robots for biomedical applications. Deep studies are still needed to upgrade these robots to meet all the requirements for real applications. On the other hand, origami structures have been widely used in aerospace engineering,<sup>[136–138]</sup> and the typical applications include foldable solar panels and antennas. However, origami robots have not been fully exploited for aerospace engineering. One possible application is to develop origami robot-based landers and rovers to explore superior planets.

## Acknowledgements

Q.G. acknowledges the financial support by the National Natural Science Foundation of China (No. 12472152) and the Program of Guangdong Province (no. 2019Q01Z438). B.J. acknowledges the financial support by the Shanghai Rising-Star Program (No. 24YF2747700) and the sponsored by Shanghai Pujiang Program (No. 24PJ1A129). L.J. acknowledges the support by the Hong Kong Research Grants Council under the Hong Kong PhD Fellowship Scheme.

## Conflict of Interest

The authors declare no conflict of interest.

## Keywords

3D printing, actuation mechanisms, fabrication techniques, origami robots, soft robotics

Received: February 11, 2025

Revised: April 26, 2025

Published online:

- [1] J. F. Engelberger, Springer Science & Business Media New York, **2012**.
- [2] S. B. Niku, *Introduction to Robotics, Analysis, Control, applications*, John Wiley & Sons, Chichester, UK **2020**.
- [3] M. Dalle Mura, G. Dini, *CIRP Ann.* **2019**, 68, 1.
- [4] H. Zhuang, H. Gao, Z. Deng, L. Ding, Z. Liu, *Sci. China Technol. Sci.* **2014**, 57, 298.
- [5] R. R. Murphy, S. Tadokoro, A. Kleiner, *Disaster Robotics*, Springer handbook of robotics, New York **2016**, pp. 1577–1604.
- [6] D. Rus, M. T. Tolley, *Nature* **2015**, 521, 467.
- [7] Y. Sun, A. Abudula, H. Yang, S.-S. Chiang, Z. Wan, S. Ozel, R. Hall, E. Skorina, M. Luo, C. D. Onal, *Current Robotics Reports* **2021**, 2, 371.
- [8] J. Shintake, V. Cacucciolo, D. Floreano, H. Shea, *Adv. Mater.* **2018**, 30, 1707035.
- [9] M. Runciman, A. Darzi, G. P. Mylonas, *Soft Rob.* **2019**, 6, 423.
- [10] A. D. Marchese, C. D. Onal, D. Rus, *Soft Rob.* **2014**, 1, 75.
- [11] M. Cianchetti, C. Laschi, A. Menciassi, Dario, *Nat. Rev. Mater.* **2018**, 3, 143.
- [12] Y. Wang, Z. Xie, H. Huang, X. Liang, *Smart Med.* **2024**, 3, 20230045.
- [13] R. Pramanik, R. Verstappen, R. Onck, *Appl. Phys. Rev.* **2024**, 11, 021312.
- [14] D. R. Yao, I. Kim, S. Yin, W. Gao, *Adv. Mater.* **2024**, 36, 2308829.
- [15] Z. Chen, Y. Wang, H. Chen, J. Law, H. Pu, S. Xie, F. Duan, Y. Sun, N. Liu, J. Yu, *Nat. Commun.* **2024**, 15.
- [16] L. Jin, X. Zhai, K. Zhang, J. Jiang, W. H. Liao, *Mater. Sci. in Addit. Manuf.* **2024**, 3, 4144.
- [17] S. Kim, C. Laschi, B. Trimmer, *Trends Biotechnol.* **2013**, 31, 287.
- [18] C. Laschi, B. Mazzolai, M. Cianchetti, *Sci. Rob.* **2016**, 1, aah3690.
- [19] M. Meloni, et al., *Adv. Sci.* **2021**, 8, 2000636.
- [20] D. Rus, C. Sung, *Sci. Rob.* **2018**, 3, aat0938.
- [21] D. Rus, M. T. Tolley, *Nat. Rev. Mater.* **2018**, 3, 101.
- [22] D.-Y. Lee, J.-K. Kim, C.-Y. Sohn, J.-M. Heo, K.-J. Cho, *Sci. Rob.* **2021**, 6, abe0201.
- [23] M. Park, W. Kim, S.-Y. Yu, J. Cho, W. Kang, J. Byun, U. Jeong, K.-J. Cho, *IEEE Robotics and Automation Letters* **2022**, 8, 864.
- [24] C. Ai, Y. Chen, L. Xu, H. Li, C. Liu, F. Shang, Q. Xia, S. Zhang, *Adv. Eng. Mater.* **2021**, 23, 2100473.
- [25] Y. Alapan, A. C. Karacakol, S. N. Guzelhan, I. Isik, M. Sitti, *Sci. Adv.* **2020**, 6, abc6414.
- [26] Y. Feng, W. Yan, J. Song, Z. Hong, H. Qiu, K. Cui, X. Song, J. Tan, *Adv. Mater. Technol.* **2024**, 9, 2301924.
- [27] G. D. Goh, G. L. Goh, Z. Lyu, M. Z. Ariffin, W. Y. Yeong, G. Z. Lum, D. Campolo, B. S. Han, H. Y. A. Wong, *Adv. Mater. Technol.* **2022**, 7, 2101672.
- [28] T. H. Kim, J. Vanloo, W. S. Kim, *Adv. Mater. Technol.* **2021**, 6, 2000938.
- [29] S. Wu, T. Zhao, Y. Zhu, G. H. Paulino, *Proc. Natl. Acad. Sci. USA* **2024**, 121, 2322625121.
- [30] W. Xue, L. Jin, B. Jian, Q. Ge, *Soft Rob.* **2025**, 0, null.
- [31] S. Leanza, S. Wu, X. Sun, H. J. Qi, R. R. Zhao, *Adv. Mater. n/a*, 2302066.
- [32] B. An, D. Rus, in 2012 IEEE Int. Con. on Robotics and Automation, IEEE, Piscataway, NJ **2012**.
- [33] H. Banerjee, N. Pusalkar, H. Ren, *J. Mech. Rob.* **2018**, 10, 064501.
- [34] S. Felton, M. Tolley, E. Demaine, D. Rus, R. Wood, *Science* **2014**, 345, 644.
- [35] A. Kotikian, C. McMahan, E. C. Davidson, J. M. Muhammad, R. D. Weeks, C. Daraio, J. A. Lewis, *Sci. Rob.* **2019**, 4, aax7044.
- [36] D.-Y. Lee, S.-R. Kim, J.-S. Kim, J.-J. Park, K.-J. Cho, *Soft Rob.* **2017**, 4, 163.
- [37] S.-J. Kim, D.-Y. Lee, G.-P. Jung, K.-J. Cho, *Sci. Rob.* **2018**, 3, aar2915.
- [38] E. V. Hoff, J. Donghwa, L. Kiju, in 2014 IEEE/RSJ Int. Conf. on Intelligent Robots and Systems, IEEE, Piscataway, NJ **2014**.
- [39] Q. Ze, S. Wu, J. Nishikawa, J. Dai, Y. Sun, S. Leanza, C. Zemelka, L. S. Novelino, G. H. Paulino, R. R. Zhao, *Sci. Adv.* **2022**, 8, abm7834.
- [40] A. Pagano, T. Yan, B. Chien, A. Wissa, S. Tawfick, *Smart Mater. Struct.* **2017**, 26, 094007.
- [41] E. Hawkes, B. An, N. M. Benbernou, H. Tanaka, S. Kim, E. D. Demaine, D. Rus, R. J. Wood, *Proc. Natl. Acad. Sci. USA* **2010**, 107, 12441.
- [42] Z. Zhakypov, F. Heremans, A. Billard, J. Paik, *IEEE Robotics and Automation Letters* **2018**, 3, 2894.
- [43] Q. Ge, C. K. Dunn, H. J. Qi, M. L. Dunn, *Smart Mater. Struct.* **2014**, 23, 094007.
- [44] B. Y. Ahn, D. Shoji, C. J. Hansen, E. Hong, D. C. Dunand, J. A. Lewis, *Adv. Mater.* **2010**, 22, 2251.
- [45] C. D. Onal, M. T. Tolley, R. J. Wood, D. Rus, *IEEE/ASME Transactions on Mechatronics* **2014**, 20, 2214.
- [46] Q. Liu, H. Ye, J. Cheng, H. Li, X. He, B. Jian, Q. Ge, *Acta Mechanica Solida Sinica* **2023**, 36, 582.
- [47] H. Ye, Q. Liu, J. Cheng, H. Li, B. Jian, R. Wang, Z. Sun, Y. Lu, Q. Ge, *Nat. Commun.* **2023**, 14, 1607.
- [48] Y. Kim, H. Yuk, R. Zhao, S. A. Chester, X. Zhao, *Nature* **2018**, 558, 274.
- [49] Z. Zhao, X. Kuang, J. Wu, Q. Zhang, G. H. Paulino, H. J. Qi, D. Fang, *Soft Matter* **2018**, 14, 8051.
- [50] S. J. Callens, A. A. Zadpoor, *Mater. Today* **2018**, 21, 241.
- [51] L. H. Dudte, E. Vouga, T. Tachi, L. Mahadevan, *Nat. Mater.* **2016**, 15, 583.
- [52] J. E. Suh, T. H. Kim, J. H. Han, *Journal of Spacecraft and Rockets* **2021**, 58, 516.
- [53] S. Zang, D. Misseroni, T. Zhao, G. H. Paulino, *J. Mech. Phys. Solids* **2024**, 188.
- [54] W. Xu, M. Zhang, H. Xu, M. Yu, L. Jin, X. Zhai, J. Jiang, *Compos. B Eng.* **2025**, 297.
- [55] Y. Gu, L. Hao, J. Zhao, W. Xing, S. Ke, Y. Yu, T. Zhang, C. Zhang, *J. Mech. Des.* **2025**, 147, 090801.
- [56] J. Li, H. Zhang, J. Long, G. Lu, *Extreme Mech. Lett.* **2025**, 75.
- [57] W. Xue, Z. Sun, H. Ye, Q. Liu, B. Jian, Y. Wang, H. Fang, Q. Ge, *Smart Mater. Struct.* **2024**, 33, 035004.
- [58] B. Chen, Z. Shao, Z. Xie, J. Liu, F. Pan, L. He, L. Zhang, Y. Zhang, X. Ling, F. Peng, W. Yun, L. Wen, *Adv. Intell. Syst.* **2021**, 3, 2000251.
- [59] Y. Kim, Y. Lee, Y. Cha, *IEEE Access* **2021**, 9, 41010.
- [60] Q. Ze, S. Wu, J. Dai, S. Leanza, G. Ikeda, C. Yang, G. Iaccarino, R. R. Zhao, *Nat. Commun.* **2022**, 13, 3118.
- [61] H. Fang, Y. Zhang, K. W. Wang, *Bioinspiration & Biomimetics* **2017**, 12, 065003.
- [62] C. Wang, H. Guo, R. Liu, H. Yang, Z. Deng, *Smart Mater. Struct.* **2021**, 30, 055010.
- [63] S. Li, J. J. Stampfli, H. J. Xu, E. Malkin, E. V. Diaz, D. Rus, R. J. Wood, in 2019 Int. Conf. on Robotics and Automation (ICRA). **2019**.
- [64] P. Zhao, C. Wu, Y. Li, *Chinese Journal of Aeronautics* **2023**, 36, 125.
- [65] J. Berre, F. Geiskopf, L. Rubbert, P. Renaud, in *New Advances in Mechanisms, Mechanical Transmissions and Robotics*, Springer International Publishing, Cham, New York **2021**.
- [66] D.-Y. Lee, J. S. Kim, S. R. Kim, J. S. Koh, K. J. Cho, in ASME 2013 Int. Design Engineering Technical Conf. and Computers and Information in Engineering Conference, **2013**.
- [67] K. Kuribayashi, K. Tsuchiya, Z. You, D. Tomus, M. Umemoto, T. Ito, M. Sasaki, *Mater. Sci. Eng., A* **2006**, 419, 131.
- [68] W. Kim, J. Byun, J. K. Kim, W. Y. Choi, K. Jakobsen, J. Jakobsen, D. Y. Lee, K. J. Cho, *Sci Robot* **2019**, 4.
- [69] J. Yi, X. Chen, C. Song, J. Zhou, Y. Liu, S. Liu, Z. Wang, *IEEE Trans. Robot.* **2018**, 35, 114.
- [70] N. Oh, H. Lee, J. Shin, Y. Choi, K. J. Cho, H. Rodrigue, *IEEE-ASME Transactions on Mechatronics* **2024**, 30, 657.
- [71] S. Li, D. M. Vogt, D. Rus, R. J. Wood, *Proc Natl Acad Sci U S A* **2017**, 114, 13132.

- [72] C. Zhang, Z. Zhang, Y. Peng, Y. Zhang, S. An, Y. Wang, Z. Zhai, Y. Xu, H. Jiang, *Nat. Commun.* **2023**, *14*, 4329.
- [73] W. Fan, J. Wang, Z. Zhang, G. Chen, H. Wang, *IEEE-ASME Transactions on Mechatronics* **2024**, *29*, 3370.
- [74] D. Jeong, K. Lee, *Robotica* **2018**, *36*, 261.
- [75] Y. Xu, Q. Peyron, J. Kim, J. Burgner-Kahrs, IEEE 4th International Conference on Soft Robotics (Robosoft), **2021**, 308–314.
- [76] J. Kim, E. Im, Y. Lee, Y. Cha, *Sensors and Actuators a-Physical* **2024**, *378*.
- [77] G. Chung, J. W. Chae, D.-S. Han, S. M. Won, Y. Park, *Adv. Intell. Syst.* **2024**, *6*, 2400082.
- [78] S. Miyashita, S. Guitron, K. Yoshida, S. Li, D. D. Damian, D. Rus, in *2016 IEEE International Conference on Robotics and Automation (ICRA)*, **2016**.
- [79] F. Gabler, D. D. Karnaushenko, D. Karnaushenko, O. G. Schmidt, *Nat. Commun.* **2019**, *10*, 3013.
- [80] Z. Zhakypov, K. Mori, K. Hosoda, J. Paik, *Nature* **2019**, *571*, 381.
- [81] C. D. Onal, R. J. Wood, D. Rus, *IEEE/ASME Transactions on Mechatronics* **2013**, *18*, 430.
- [82] J. Wang, H. Yang, J. Zhang, H. Liu, Y. Zhong, Y. Hu, Y. Liu, C. Xia, J. Wu, *Adv. Intell. Syst.* **2025**, 2401008.
- [83] Y. Jin, J. Li, S. Liu, G. Cao, J. Liu, *Bioinspiration & Biomimetics* **2023**, *18*.
- [84] D. Tang, C. Zhang, H. Sun, H. Dai, J. Xie, J. Fu, P. Zhao, *Nano Energy* **2021**, *89*.
- [85] S. Yuan, S. Cao, J. Xue, S. Su, J. Yan, M. Wang, W. Yue, S. S. Cheng, J. Liu, J. Wang, S. Song, M. Q.-H. Meng, H. Ren, *IEEE Robotics and Automation Letters* **2022**, *7*, 10486.
- [86] Q. Ge, H. J. Qi, M. L. Dunn, *Appl. Phys. Lett.* **2013**, *103*, 131901.
- [87] Q. Ge, C. K. Dunn, H. J. Qi, M. L. Dunn, *Smart Mater. Struct.* **2014**, *23*, 094007.
- [88] C. Yuan, T. Wang, M. L. Dunn, H. J. Qi, *International Journal of Precision Engineering and Manufacturing-Green Technology* **2017**, *4*, 281.
- [89] H. Li, Z. Chen, S. Yu, B. Jian, H. Yin, Q. Ge, *Programmable Materials* **2024**, *2*, 6.
- [90] Y. Sun, D. Li, M. Wu, Y. Yang, J. Su, T. Wong, K. Xu, Y. Li, L. Li, X. Yu, J. Yu, *Microsyst. Nanoeng.* **2022**, *8*, 37.
- [91] X. Yin, P. Zhou, S. Wen, J. Zhang, *IEEE Trans. Instrum. Meas.* **2022**, *71*.
- [92] Y. Li, T. Zhang, *IEEE Robotics and Automation Letters* **2022**, *7*, 11775.
- [93] Y. Mao, K. Yu, M. S. Isakov, J. Wu, M. L. Dunn, H. Jerry Qi, *Sci. Rep.* **2015**, *5*, 14139.
- [94] Q. Ge, A. H. Sakhaii, H. Lee, C. K. Dunn, N. X. Fang, M. L. Dunn, *Sci. Rep.* **2016**, *6*, 24802.
- [95] Q. Ze, X. Kuang, S. Wu, J. Wong, S. M. Montgomery, R. Zhang, J. M. Kovitz, F. Yang, H. J. Qi, R. Zhao, *Adv. Mater.* **2020**, *32*, 1906657.
- [96] K. Zhang, J. Jiang, L. Jin, Q. Gao, X. Zhai, S. Zhou, Z. Li, J. Li, W.-H. Liao, *Smart Mater. Struct.* **2025**, *34*, 045025.
- [97] K. Zheng, E. Gao, B. Tian, J. Liang, Q. Liu, E. Xue, Q. Shao, W. Wu, *Adv. Intell. Syst.* **2022**, *4*, 2100280.
- [98] P. Velvaluri, A. Soor, Plucinsky, R. L. de Miranda, R. D. James, E. Quandt, *Sci. Rep.* **2021**, *11*, 10988.
- [99] K. Kurabayashi, K. Tsuchiya, Z. You, D. Tomus, M. Umemoto, T. Ito, M. Sasaki, *Mater. Sci. Eng.* **2006**, *419*, 131.
- [100] G. Li, X. Chen, F. Zhou, Y. Liang, Y. Xiao, X. Cao, Z. Zhang, M. Zhang, B. Wu, S. Yin, Y. Xu, H. Fan, Z. Chen, W. Song, W. Yang, B. Pan, J. Hou, W. Zou, S. He, X. Yang, G. Mao, Z. Jia, H. Zhou, T. Li, S. Qu, Z. Xu, Z. Huang, Y. Luo, T. Xie, J. Gu, et al., *Nature* **2021**, *591*, 66.
- [101] R. Brito-Pereira, C. Ribeiro, A. G. Díez, V. F. Cardoso, C. Klapperich, S. Lanceros-Mendez, P. Martins, *Appl. Mater. Today* **2024**, *40*, 102352.
- [102] S. Jiang, B. Li, J. Zhao, D. Wu, Y. Zhang, Z. Zhao, Y. Zhang, H. Yu, K. Shao, C. Zhang, R. Li, C. Chen, Z. Shen, J. Hu, B. Dong, L. Zhu, J. Li, L. Wang, J. Chu, Y. Hu, *Nat. Commun.* **2023**, *14*, 5455.
- [103] K. Han, C. W. Shields, N. M. Diwakar, B. Bharti, G. P. López, O. D. Velev, *Sci. Adv.* **2017**, *3*, 1701108.
- [104] B. Jin, H. Song, R. Jiang, J. Song, Q. Zhao, T. Xie, *Sci. Adv.* **2018**, *4*, eaao3865.
- [105] H. Gao, J. Li, Y. Liu, J. Leng, *Advanced Composites and Hybrid Materials* **2021**, *4*, 957.
- [106] A. Li, P. Cuvin, S. Lee, J. Gu, C. Tugui, M. Duduta, *Adv. Funct. Mater.* **2024**, *34*.
- [107] O. Angatkina, B. Chien, A. Pagano, T. Yan, A. Alleyne, S. Tawfick, A. Wissa, *Proceedings of the Asme Conference on Smart Materials, Adaptive Structures and Intelligent Systems* **2017**, *1*, 2017.
- [108] J. A. Faber, A. F. Arrieta, A. R. Studart, *Science* **2018**, *359*, 1386.
- [109] D. Melancon, A. E. Forte, L. M. Kamp, B. Gorissen, K. Bertoldi, *Adv. Funct. Mater.* **2022**, *32*, 2201891.
- [110] Y. Wang, H. Ye, J. He, Q. Ge, Y. Xiong, *Nat. Commun.* **2024**, *15*, 1838.
- [111] J. A. Lewis, *Adv. Funct. Mater.* **2006**, *16*, 2193.
- [112] P. Cao, J. Yang, J. Gong, L. Tao, T. Wang, X. Pei, Q. Wang, Y. Zhang, *Adv. Mater. Technol.* **2024**, *9*, 2301904.
- [113] G. Liu, Y. Zhao, G. Wu, J. Lu, *Sci. Adv.* **2018**, *4*, aat0641.
- [114] M. A. Skylar-Scott, J. Mueller, C. W. Visser, J. A. Lewis, *Nature* **2019**, *575*, 330.
- [115] K. Lee, Y. Wang, C. Zheng, *IEEE Transactions on Robotics* **2020**, *36*, 488.
- [116] P. Huang, H. Fu, M. W. M. Tan, Y. Jiang, S. Lee, *Adv. Mater. Technol.* **2024**, *9*, 2301642.
- [117] Z. Zhao, J. Wu, X. Mu, H. Chen, H. J. Qi, D. Fang, *Sci. Adv.* **2017**, *3*, 1602326.
- [118] J. Cheng, R. Wang, Z. Sun, Q. Liu, X. He, H. Li, H. Ye, X. Yang, X. Wei, Z. Li, B. Jian, W. Deng, Q. Ge, *Nat. Commun.* **2022**, *13*, 7931.
- [119] H. Li, B. Zhang, H. Ye, B. Jian, X. He, J. Cheng, Z. Sun, R. Wang, Z. Chen, J. Lin, R. Xiao, Q. Liu, Q. Ge, *Sci. Adv.* **2024**, *10*.
- [120] B. Jian, H. Li, X. He, R. Wang, H. Y. Yang, Q. Ge, *International Journal of Extreme Manufacturing* **2024**, *6*, 012001.
- [121] C. Amruth, A. K. Singh, A. Sharma, D. Corzo, D. Baran, *Adv. Mater. Technol.* **2024**, *9*, 2400290.
- [122] Z. Lin, L. S. Novelino, H. Wei, N. A. Alderete, G. H. Paulino, H. D. Espinosa, S. Krishnaswamy, *Small* **2020**, *16*, 2002229.
- [123] H. Ceylan, I. C. Yasa, O. Yasa, A. F. Tabak, J. Giltinan, M. Sitti, *ACS Nano* **2019**, *13*, 3353.
- [124] T.-Y. Huang, H.-W. Huang, D. D. Jin, Q. Y. Chen, J. Y. Huang, L. Zhang, H. L. Duan, *Sci. Adv.* **2020**, *6*, eaav8219.
- [125] D. Jin, Q. Chen, T.-Y. Huang, J. Huang, L. Zhang, H. Duan, *Mater. Today* **2020**, *32*, 19.
- [126] L. Jin, S. Yu, J. Cheng, H. Ye, X. Zhai, J. Jiang, K. Zhang, B. Jian, M. Bodaghi, Q. Ge, W. H. Liao, *Appl. Mater. Today* **2024**, *40*, 102373.
- [127] L. Jin, S. Yu, J. Cheng, Z. Liu, K. Zhang, S. Zhou, X. He, G. Xie, M. Bodaghi, Q. Ge, W. H. Liao, *Composites Part B-Engineering* **2025**, *299*, 112372.
- [128] L. Jin, X. Zhai, J. Jiang, K. Zhang, W. H. Liao, in *Sensors and Smart Structures Technologies for Civil, Mechanical, and Aerospace Systems*, SPIE, Bellingham, WA, **2024**, pp. 321—332.
- [129] L. Jin, X. Zhai, J. Jiang, K. Zhang, W. H. Liao, *Smart Mater. Struct.* **2025**, *34*, 033002.
- [130] L. Jin, X. Zhai, K. Wang, K. Zhang, D. Wu, A. Nazir, J. Jiang, W. H. Liao, *Mater. Des.* **2024**, *244*, 113086.
- [131] L. H. Dudte, G. P. T. Choi, L. Mahadevan, *Proc. Natl. Acad. Sci. USA* **2021**, *118*, e2019241118.
- [132] K. Xiao, Z. Liang, B. Zou, X. Zhou, J. Ju, *Nat. Commun.* **2022**, *13*, 7474.
- [133] A. R. Ahmed, O. C. Gauntlett, G. Camci-Unal, *ACS Omega* **2020**, *6*, 46.

- [134] V. A. Bolaños Quiñones, H. Zhu, A. A. Solovev, Y. Mei, D. H. Gracias, *Adv. Biosyst.* **2018**, *2*, 1800230.
- [135] M. Johnson, Y. Chen, S. Hovet, S. Xu, B. Wood, H. Ren, J. Tokuda, Z. T. H. Tse, *Int. J. Comput. Assist. Radiol. Surg* **2017**, *12*, 2023.
- [136] K. F. Hussain, W. J. Cantwell, K. A. Khan, *Proceedings of ASME 2023 Int. Mech. Eng. Congress and Exposition* **2023**, 87615, V004T05A006.
- [137] J. Morgan, S. P. Magleby, L. L. Howell, *J. Mech. Des.* **2016**, *138*, 052301.
- [138] S. Yue, in *Journal of Physics, Conference Series*, IOP Publishing **2023**.



**Wenbo Xue** is a Ph.D. student in the Department of Mechanical and Energy Engineering at Southern University of Science and Technology (SUSTech), under the supervision of Prof. Qi Ge. His research interests include origami robots, soft robotics, and smart materials and structures. He received his bachelor's degree from Northwest University (NWU) in 2019. He has been recognized with a Certificate of Achievement and an Honorable Mention in the Mathematical Contest in Modeling (MCM), and won the Second Prize in the 12th National Chemical Engineering Design Competition for College Students.



**Bingcong Jian** is an assistant professor at the School of Mechanical Engineering at Tongji University. She obtained her bachelor's degree in Aircraft Design and Engineering from Northwestern Polytechnical University, a master's degree in Mechanical Design, and an engineering degree from the National Institute of Applied Sciences of Lyon, France. She was awarded a CSC sponsorship to conduct research at the University of Burgundy-Franche-Comté, France, where she earned her Ph.D. in Mechanical Engineering. Dr. Jian undertakes postdoctoral research at Southern University of Science and Technology. Her research focused on 4D printing technology, origami structure design, and the application of intelligent materials.



**Liuchao Jin** is a Ph.D. candidate in the Department of Mechanical and Automation Engineering at The Chinese University of Hong Kong (CUHK) supervised by Prof. Wei-Hsin Liao. He is a recipient of Hong Kong PhD Fellowship Scheme (HKPFS). He is also a visiting student at the Southern University of Science and Technology (SUSTech). His research focuses on 3D/4D printing, smart materials and structures, and soft robotics. Liuchao obtained bachelor's degree from the Sichuan University – Pittsburgh Institute (SCUPI). He has also gained research experience as a Mitacs Globalink Research Intern at McGill University and a Research Assistant at Westlake University.



**Rong Wang** is a research assistant professor in the Department of Mechanical and Energy Engineering at Southern University of Science and Technology (SUSTech). He received his Ph.D. from the University of Chinese Academy of Sciences in 2018, and then conducted postdoctoral research at Tsinghua Shenzhen International Graduate School. He joined SUSTech in 2020. His research focuses on DLP-based 3D/4D printing, multimaterial additive manufacturing, and multifunctional structures and devices.



**Qi Ge** is a professor and associate dean at the Department of Mechanical and Energy Engineering, Southern University of Science and Technology. He also serves as director of Shenzhen Key Laboratory for Additive Manufacturing of High-Performance Materials. He has worked as a postdoctoral researcher at the Massachusetts Institute of Technology and as an assistant professor at the Singapore University of Technology and Design. His research focuses on smart materials, 4D printing, soft robotics, and flexible electronics. He serves on the editorial boards of journals including *International Journal of Extreme Manufacturing* and *Microsystems & Nanoengineering*.